

Strong to weak coupling transitions of $SU(N)$ gauge theories in $2+1$ dimensions

Francis Bursa and Michael Teper

Rudolf Peierls Centre for Theoretical Physics, University of Oxford,
1 Keble Road, Oxford OX1 3NP, U.K.

Abstract

We investigate strong-to-weak coupling transitions in $D = 2 + 1$ $SU(N \rightarrow \infty)$ gauge theories, by simulating the corresponding lattice theories with a Wilson plaquette action. We find that there is a strong-to-weak coupling cross-over in the lattice theory that appears to become a third-order phase transition at $N = \infty$, in a manner that is essentially identical to the Gross-Witten transition in the $D = 1 + 1$ $SU(\infty)$ lattice gauge theory. There is evidence of an additional second order transition developing at $N = \infty$ at approximately the same coupling, which is connected with Z_N monopoles (instantons), thus making it an analogue of the first order bulk transition that occurs in $D = 3 + 1$ lattice gauge theories for $N \geq 5$. We show that as the lattice spacing is reduced, the $N = \infty$ gauge theory on a finite 3-torus suffers a sequence of (apparently) first-order Z_N symmetry breaking transitions associated with each of the tori (ordered by size). We discuss how these transitions can be understood in terms of a sequence of deconfining transitions on ever-more dimensionally reduced gauge theories. We investigate whether the trace of the Wilson loop has a non-analyticity in the coupling at some critical area, but find no evidence for this. However we do find that, just as one can prove occurs in $D = 1 + 1$, the eigenvalue density of a Wilson loop forms a gap at $N = \infty$ at a critical value of its trace. The physical implications of this subtle non-analyticity are unclear. This gap formation is in fact a special case of a remarkable similarity between the eigenvalue spectra of Wilson loops in $D = 1 + 1$ and $D = 2 + 1$ (and indeed $D = 3 + 1$): for the same value of the trace, the eigenvalue spectra are nearly identical. This holds for finite as well as infinite N ; irrespective of the Wilson loop size in lattice units; and for Polyakov as well as Wilson loops.

1 Introduction

A phase transition is associated with a singularity in the partition function, and so requires an infinite number of degrees of freedom. Usually that requires an infinite volume. One of the peculiarities of large- N field theories is that one can have phase transitions on finite, or even infinitesimal, volumes at $N = \infty$ because in this case we have an infinite number of degrees of freedom at each point in space. The classic example in the context of gauge field theories is the Gross-Witten transition [1] that occurs in the $D = 1 + 1$ $SU(\infty)$ lattice gauge theory (with the standard Wilson action). In this case the theory is analytically soluble and one finds a third order phase transition at $N = \infty$ [1] at a value of the bare coupling that separates the strong and weak coupling regions. The theoretical and practical interest of such phase transitions, particularly in $D = 3 + 1$, has recently been reviewed in [2].

In $D = 3 + 1$ $SU(N)$ gauge theories numerical studies reveal the existence for $N \geq 5$ of a first order ‘bulk’ transition separating the weak and strong coupling regions [3, 4, 5]. One also finds that the deconfinement transition, which is first order for $N \geq 3$, becomes sharper on smaller volumes as N increases suggesting [6] that here too one will have a phase transition on a finite volume at $N = \infty$. Indeed there appears to be a whole hierarchy of finite volume phase transitions at $N = \infty$ [7, 2] which are, we shall argue below, related to the deconfinement transition.

These are all in some sense strong to weak coupling transitions, and this has led to the conjecture [8, 2] that Wilson loops in general will show such $N = \infty$ transitions as the lattice spacing decreases, when the physical size of the loop passes some critical value. Such a transition in $D = 3 + 1$ could have interesting implications for dual string approaches to large- N gauge theories, as well as providing a natural explanation for the rapid crossover between perturbative and non-perturbative physics that is observed in the strong interactions [1, 11, 2]. In fact it is known [9, 10] that in the $N = \infty$ $D = 1 + 1$ continuum theory the eigenvalue spectrum of a Wilson loop suffers a non-analyticity for a critical area that is very similar to that of the plaquette at the Gross-Witten transition. However, in contrast to the Gross-Witten transition, there is no accompanying non-analyticity in the trace of the loop and it is unclear what, if any, are its physical implications.

In this paper we investigate the existence of such phase transitions in $D = 2 + 1$ $SU(N)$ gauge theories, as a step towards a unified understanding of these phenomena in all dimensions.

In the next Section we briefly describe the $SU(N)$ lattice gauge theory and how we simulate it. There follows a longer section in which we review in more detail what is known about the large- N transitions and, in some cases, we extend the analysis. (We are interested in transitions that may be cross-overs or actual phase transitions, and when we refer to ‘transitions’ in this paper it may be either one of these.) Having established the background, we move on to our detailed numerical results. Our conclusions contain a summary of our main results.

2 $SU(N)$ gauge theory on the lattice

We discretise Euclidean space-time to a periodic cubic lattice with lattice spacing a and size $L_0 \times L_1 \times L_2$ in lattice units. We assign $SU(N)$ matrices, U_l , to the links l of the lattice. (We sometimes write U_l as $U_\mu(n)$ where the link l emanates in the positive μ direction from the site n .) We use the standard Wilson plaquette action

$$S = \beta \sum_p \left\{ 1 - \frac{1}{N} \text{ReTr} U_p \right\} \quad (1)$$

where U_p is the ordered product of the $SU(N)$ link matrices around the boundary of the plaquette p . The partition function is

$$Z = \int \prod_l dU_l \exp(-S) \quad ; \quad \lim_{a \rightarrow 0} \beta = \frac{2N}{ag^2}. \quad (2)$$

Exactly the same expression defines the lattice gauge theory in $D = 1+1$ and $D = 3+1$ except that $\beta = 2N/a^2g^2$ and $\beta = 2N/g^2$ respectively. Eqn(2) also defines the finite temperature partition function, if we choose

$$T = \frac{1}{aL_0} \quad ; \quad L_1, L_2 \gg L_0. \quad (3)$$

We simulate the above lattice theory using a conventional mixture of heat bath and over-relaxation steps applied to the $SU(2)$ subgroups of the $SU(N)$ link matrices.

It will sometimes be convenient to distinguish couplings, inverse bare couplings and (critical) temperatures in different space-time dimensions, D , and we do so using subscripts or superscripts, e.g. g_D^2 , β_D , T_c^D . Where there is no ambiguity we will often omit such subscripts.

To obtain a smooth large N limit we keep g^2N fixed [12]. It is therefore useful to define the bare 't Hooft coupling, λ , and the inverse bare 't Hooft coupling, γ ,

$$\lambda = ag^2N \quad , \quad \gamma = \frac{1}{\lambda} = \frac{\beta}{2N^2}. \quad (4)$$

Various numerical calculations have confirmed that a smooth $N \rightarrow \infty$ limit is indeed obtained by keeping λ fixed, both in $D = 2 + 1$ [13] and in $D = 3 + 1$ [4, 6, 14] and that to keep the cut-off a fixed as $N \rightarrow \infty$ one should keep γ fixed.

A useful order parameter for finite volume phase transitions is provided by taking the Polyakov loop, l_μ , which is the ordered product of link matrices around the μ -torus, and averaging it over the space-time volume:

$$\bar{l}_\mu = c_\mu \sum_{n_\nu \neq \mu} \frac{1}{N} \text{Tr} \left\{ \prod_{n_\mu=1}^{n_\mu=L_\mu} U_\mu(n_0, n_1, n_2) \right\} \quad (5)$$

where the normalisation is $c_\mu^{-1} = \prod_{\nu \neq \mu} L_\nu$. When the system develops a non-zero value for $\langle \bar{l}_\mu \rangle$ this indicates the spontaneous breaking of a global Z_N symmetry associated with the μ -torus. In particular such a symmetry breaking occurs at the deconfining temperature, if the μ -torus defines the temperature T .

3 Background

3.1 The ‘Gross-Witten’ transition

By fixing gauge and making a change of variables, one can show [1] that the partition function of the $D = 1 + 1$ $SU(N)$ lattice gauge theory (with the Wilson plaquette action) factorises into a product of integrals over $SU(N)$ matrices on the links and the theory can be explicitly solved. One then finds a cross-over between weak and strong coupling that sharpens with increasing N into a third order phase transition at $N = \infty$. In terms of the plaquette, $u_p = \text{ReTr} U_p / N$, this shows up in a change of functional behaviour

$$\langle u_p \rangle \stackrel{N \rightarrow \infty}{=} \begin{cases} \frac{1}{\lambda} & \lambda \geq 2, \\ 1 - \frac{\lambda}{4} & \lambda \leq 2. \end{cases} \quad (6)$$

More detailed information about the behaviour of plaquettes and Wilson loops can be gained by considering not just their traces but their eigenvalues. The eigenvalues of an $SU(N)$ matrix are just phases, $\lambda = \exp\{i\alpha\}$, and are gauge-invariant. (We also use λ for the ‘t Hooft coupling: which is intended should be clear from the context.) As $\beta \rightarrow 0$ the eigenvalue distribution $\rho(\alpha)$ of a Wilson loop becomes uniform while as $\beta \rightarrow \infty$ it becomes increasingly peaked around $\alpha = 0$. As shown in [1], at the Gross-Witten transition a gap opens in the density of plaquette eigenvalues: in the strongly-coupled phase the eigenvalue density is non-zero for all angles $-\pi \leq \alpha \leq \pi$, but in the weakly-coupled phase it is only non-zero in the range $-\alpha_c \leq \alpha \leq \alpha_c$, where $\alpha_c < \pi$ [1].

In $D = 3 + 1$ it is known that at $N = \infty$ [3], and indeed for $N \geq 5$ [4, 5], there is a strong first order transition as β is varied from strong to weak coupling. Calculations in progress [15] suggest that the plaquette eigenvalue distribution does indeed show a gap formation at $N = \infty$ that is similar to the $D = 1 + 1$ Gross-Witten transition. However the first order transition itself is usually believed to be a manifestation of the phase structure one finds with a mixed adjoint-fundamental action as discussed below. This finite- N phase transition ‘conceals’ any underlying $N = \infty$ Gross-Witten transition and makes the latter hard to identify unambiguously.

In $D = 2 + 1$ there has been, as far as we are aware, no systematic search for a Gross-Witten or ‘bulk’ transition, and this is one of the gaps that the present work intends to fill.

3.2 Wilson loop transitions

The Gross-Witten transition involves the smallest possible Wilson loop, the plaquette. On the weak coupling side the plaquette can be calculated in terms of usual weak-coupling perturbation theory; but this breaks down abruptly at the Gross-Witten transition, beyond which a strong coupling expansion becomes appropriate [1]. The coupling is the bare coupling and hence a coupling on the length scale of the plaquette. Thus one might interpret the transition as saying that as one increases the length scale, there is a critical scale at which perturbation theory in the running coupling will suddenly break down.

One might imagine that this generalises to other Wilson loops: i.e. when we scale up a Wilson loop, at some critical size, in ‘physical units’, there is a non-analyticity. In fact precisely such a scenario has been conjectured for $SU(N \rightarrow \infty)$ gauge theories in $D = 3 + 1$ [8, 2]. Unlike the lattice Gross-Witten transition, this would be a property of the continuum theory.

Such a non-analyticity does in fact occur for the $SU(N \rightarrow \infty)$ continuum theory in $D = 1 + 1$ [9, 10]. The transition occurs at a fixed physical area

$$A_{crit} = \frac{8}{g^2 N}. \quad (7)$$

Very much larger Wilson loops have a flat eigenvalue spectrum $\rho(\alpha)$ which becomes peaked as $A \rightarrow A_{crit}^+$. As A decreases through A_{crit} a gap appears in the spectrum near the extreme phases $\alpha = \pm\pi$. So for loops with $A < A_{crit}^+$ the eigenvalue density is only non-zero for $-\alpha_c \leq \alpha \leq \alpha_c$, where $\alpha_c < \pi$, and $\alpha_c \rightarrow 0$ as $A \rightarrow 0$. The non-analyticity at $A = A_{crit}$ is in fact more singular than for the Gross-Witten transition, in that the derivative $\partial\rho/\partial\alpha$ diverges at $\alpha_c = \pm\pi$. However, unlike the Gross-Witten transition this is not a phase transition: the partition function is analytic. Moreover the trace of the Wilson loop, and the traces of all powers of the Wilson loop, remain analytic in the coupling. Thus it is unclear what if any is the physical significance of this non-analyticity.

In this paper we shall investigate whether such a non-analyticity develops in $D = 2 + 1$ $SU(N)$ gauge theories and whether it is accompanied by any non-analyticity of the trace. The implications could be very interesting [11] and this makes a search in $D = 2 + 1$ (and even more so in $D = 3 + 1$ [15]) well worth while.

3.3 Mixed actions

In $D = 3 + 1$ the strong-to-weak coupling transition occurs already at finite N . It is a cross-over for $N \leq 4$ and is first order for $N \geq 5$ [4, 5]. The conventional interpretation of this ‘bulk’ transition proceeds by considering a generalised lattice action containing pieces in both fundamental and adjoint representations [16]:

$$\begin{aligned} S &= \beta_f \sum_p \left\{ 1 - \frac{1}{N} \text{ReTr}_f U_p \right\} + \beta'_a \sum_p \left\{ 1 - \frac{1}{N^2 - 1} \text{Tr}_a U_p \right\} \\ &= \beta_f \sum_p \left\{ 1 - \frac{1}{N} \text{ReTr}_f U_p \right\} + \beta_a \sum_p \left\{ 1 - \frac{1}{N^2} \text{Tr}_f U_p^\dagger \text{Tr}_f U_p \right\} \end{aligned} \quad (8)$$

where we have used $\text{Tr}_a U_p = |\text{Tr}_f U_p|^2 - 1$. By considering smooth fields one finds that at weak coupling, and to leading order in g^2 , one obtains constant physics by keeping constant the linear combination $\beta_f + 2\beta_a$.

Consider the limit $\beta_a \rightarrow \infty$ while keeping β_f fixed. This requires $|\text{Tr}_f U_p|^2/N^2 = 1$ which implies that the link matrices are elements of the centre. Fluctuations between different elements of the centre are controlled by the linear plaquette term multiplied by β_f which

means that what we have is a Z_N gauge theory with coupling $\beta = \beta_f$. When $N \rightarrow \infty$ at fixed β_f , this becomes a $U(1)$ gauge theory. In $D = 3 + 1$ this theory has a strong coupling confining phase that is separated from a weak coupling Coulomb phase by a phase transition (probably first order) at $\beta_c = O(1)$ and a ‘freeze-out’ transition at $\beta'_c = O(N^2)$ where fluctuations between neighbouring elements of the centre become improbably small. These phase transitions will extend from $\beta_a = \infty$ to some finite β_a . In addition numerical calculations suggest that there is a first order line that crosses the β_f -axis (for $N \geq 5$, at the bulk transition) and also the β_a -axis (apparently for all N) and to which the first order line from β_c is attached. This phase diagram has been explored in some detail for $SU(2)$ [17] and $SU(3)$ [18]. One can interpret this phase structure in terms of the condensation of Z_N monopoles and vortices [19]. These involve large plaquette values and so the first order bulk transition involves a large jump in the average plaquette. It appears, not surprisingly, that the would-be third-order Gross-Witten transition is subsumed in this jump [15].

By contrast, in the analytically tractable case of $D = 1 + 1$, the $\lim_{N \rightarrow \infty} Z_N \sim U(1)$ theory at $\beta_a = \infty$ will have no finite- β phase transition by the same arguments used in [1] for $SU(N < \infty)$ gauge theories. One can also readily show that the finite- N cross-over along the β_f axis, which becomes the Gross-Witten transition at $N = \infty$, is matched by a similar cross-over and $N = \infty$ transition along the β_a axis. Indeed using the same change of variables and notation as in [1] one sees that $Z(\beta_f = 0, \beta_a) = z_a^V$ where $V = L_0 L_1$ and

$$\begin{aligned} z_a &= \int dW \exp\left\{\frac{\beta_a}{N^2} \text{Tr}_f W^\dagger \text{Tr}_f W\right\} \\ &= \frac{1}{1 - \frac{\beta_a}{N^2}}. \end{aligned} \tag{9}$$

Here we have expanded the exponential and then used eqn(41) of [1] which is valid for $N \rightarrow \infty$. (This argument is casual with limits and is at most valid coming from the strong coupling side [1].) Now

$$\begin{aligned} \langle \text{Tr}_a U_p + 1 \rangle &= \langle |\text{Tr}_f U_p|^2 \rangle = \langle |\text{Tr}_f W|^2 \rangle \\ &= \frac{\partial}{\partial \frac{\beta_a}{N^2}} \log z_a \\ &= \frac{1}{1 - \frac{\beta_a}{N^2}}. \end{aligned} \tag{10}$$

Clearly as we increase β_a from strong coupling there must be some non-analyticity in $\langle \text{Tr}_a U_p \rangle$ at or before the value $\beta_a/N^2 = 1$. The corresponding non-analyticity in $Z = z_a^V$ represents a phase transition. For a precise derivation we refer to [20].

In $D = 2 + 1$ the $\lim_{N \rightarrow \infty} Z_N \sim U(1)$ gauge theory at $\beta_a = \infty$ has no phase transition at finite β and is linearly confining at all β due to the the plasma of $U(1)$ monopole-instantons. In the Z_N theory there is freeze-out transition at some $\beta = O(N^2)$ [21]. Numerical calculations in $SU(2)$ [22] suggest that the line of phase transitions descending from this point into the finite β_a plane ends before reaching the $\beta_a = 0$ axis, so that there is only a peak in the specific

heat, but no phase transition, on the β_f axis. So all this suggests – albeit on limited evidence – that at finite N the $D = 2 + 1$ (β_a, β_f) phase diagram contains only smooth cross-overs (except for the freeze-out transitions), much like $D = 1 + 1$ and in contrast to the finite- N phase transitions in $D = 3 + 1$. In this paper we shall show that this is indeed the case along the β_f axis.

3.4 Finite volume transitions

Consider a $D = 3 + 1$ $SU(N)$ gauge theory on a $L_0 L^3$ lattice where $L_0 \ll L$. If we increase β from small values, then we will encounter a deconfining transition at $a(\beta)L_0 = 1/T_c$ (first order for $N \geq 3$ and second order for $N = 2$ [6, 5]). A convenient order parameter for this transition is the Polyakov loop, $\langle \bar{l}_{\mu=0} \rangle$, which acquires a non-zero expectation value in the deconfined phase. The transition is a crossover for finite L and sharpens to a phase transition as $L \rightarrow \infty$. As $N \uparrow$ the transition becomes sharper on ever smaller volumes [6, 5]. so that as $N \rightarrow \infty$ one will have a deconfining phase transition for $L = L_0 + \epsilon$ where $\epsilon > 0$ is as small as we like. By continuity one would expect an $N = \infty$ phase transition even as $\epsilon \rightarrow 0$, i.e. on an L^4 lattice. (Finessing any subtleties about orders of limits.)

This makes contact with calculations [7, 8] that have shown that if we are on a L^4 lattice and increase β , then there will be a crossover, sharpening to a phase transition at $N = \infty$, which is characterised by one of the Polyakov loops, $\langle l_\mu \rangle$, with μ chosen at random, acquiring a non-zero expectation value. In fact one finds [7, 8] that this is only the first of a sequence of phase transitions. At a second higher value of β there is a second phase transition where another Polyakov loop, $\langle l_\nu \rangle$ with $\nu \neq \mu$ again chosen at random, acquires a non zero expectation value. And there is some evidence that as β is increased further there are similar transitions along a third and fourth direction [7, 8]. Moreover one finds [7, 8] that these transitions are associated with a gap forming in the eigenvalue spectrum of the appropriate Polyakov loop, just as one finds for the plaquette at the Gross-Witten transition. It is therefore natural to think of these finite-volume transitions as being in some sense strong-to-weak coupling transitions.

As we argued above, the first of these $N = \infty$ transitions appears to be nothing but the $N = \infty$ deconfining transition and should occur at $\beta = \beta_{c_0}$ where

$$a(\beta_{c_0})L_0 = 1/T_c^{D=4}. \quad (11)$$

One can make analogous arguments for the existence of a sequence of transitions on an $L_0 L_1 L_2 L_3$ lattice with $L_0 \ll L_1 \ll L_2 \ll L_3$. To see this, consider the following steps.

(1) Increase $\beta_4 \equiv \beta$ to very high temperatures, $T = 1/a(\beta)L_0 \gg T_c$. In this regime we will have the familiar dimensional reduction to an effective $D = 2 + 1$ $SU(N)$ gauge theory coupled to adjoint scalars ϕ that are the time-translationally invariant remnant of the A_0 gauge field [23]. To leading order the gauge coupling and mass of the scalar of the effective $D = 2 + 1$ gauge-scalar theory are [23]

$$g_3^2 = g_4^2(T)T \quad ; \quad m_a^2 \propto g_4^2(T)T^2. \quad (12)$$

So $m_a/g_3^2 = O(1/g_4(T))$ and at high enough T the $D = 3 + 1$ gauge theory reduces to the $SU(N)$ gauge theory in $D = 2 + 1$ on a $L_1 \ll L_2, L_3$ lattice. As we increase $\beta_4 = \beta$ we

simultaneously increase $\beta_3 \equiv 2N/ag_3^2 \simeq \beta_4 L_0$ (neglecting the difference between $g_4^2(a^{-1})$ and $g_4^2(T)$). This $D = 2 + 1$ gauge theory will deconfine at

$$a(\beta_{c_1})L_1 = 1/T_c^{D=3} \quad (13)$$

at which point $\langle l_{\mu=1} \rangle$ acquires a non-zero vacuum expectation value. We can estimate the corresponding critical value of $\beta(\equiv \beta_4)$ to be

$$\beta_{c_1} \sim 0.36N^2 \frac{L_1}{L_0}. \quad (14)$$

To arrive at this estimate we use $(T_c/\sqrt{\sigma})_{D=3} \sim 0.9$ [24] and $\sqrt{\sigma}/g_3^2 N \simeq 0.198$ [13], together with eqn(12). For finite N this will be a cross-over, but we expect (for the same reasons as in one higher dimension) that as $N \rightarrow \infty$ one will have a phase transition on any volume where $L_2, L_3 = L_1 + \epsilon$, for any fixed ϵ however small. In the limit we thus expect the transition on a symmetric $L_0 L_1^3$ lattice with $L_1 \gg L_0$. If we now reduce L_1/L_0 then we see from eqn(14) that β_{c_1} will begin to decrease. However long before its value reaches β_{c_0} the value of T will have become small enough that we cannot neglect the adjoint scalar (and its self-interactions) and our estimate in eqn(14) ceases to be useful. Nonetheless it appears plausible that the second $N = \infty$ transition that has been observed on L^4 lattices [7, 8] is the continuation as $L_1 \rightarrow L_0$ of this three-dimensional deconfinement transition.

(2) As we increase β beyond β_{c_1} on our $L_0 \ll L_1 \ll L_2 \ll L_3$ lattice, $T^{D=3} = 1/aL_1$ will become ever larger, and eventually the system will undergo a further dimensional reduction to a $D = 1 + 1$ $SU(N)$ gauge theory with adjoint scalars [25]. To leading order the gauge coupling and scalar mass of this effective $D = 1 + 1$ gauge-scalar theory are [25]

$$g_2^2 = g_3^2 T^{D=3} \quad ; \quad m_a^2 \propto g_2^2 \log(aT^{D=3}). \quad (15)$$

While the pure gauge $D = 1 + 1$ theory has no propagating degrees of freedom and is too trivial to deconfine, the presence of the adjoint scalars renders it a non-trivial confining field theory which we would naively expect to deconfine at some $T_c^{D=2} = 1/a(\beta_{c_2})L_2$. We estimate the corresponding critical value of the coupling $\beta(\equiv \beta_4)$ to be

$$\beta_{c_2} \sim 0.43r^2 N^2 \frac{L_2^2}{L_0 L_1} \quad ; \quad r = \frac{T_c^{D=2}}{\sqrt{\sigma}} \quad (16)$$

using the value $\sigma \sim (0.8)^2 g_3^2 T N / 3$ extracted from [25]. Because we are in $D = 1 + 1$ the high- T phase cannot have a true non-zero expectation value for $\langle l_{\mu=2} \rangle$, as will be discussed more explicitly when we come to our numerical calculations below. Again we would expect that at $N = \infty$ this deconfining transition will appear on lattices with finite L_3 and even as $L_3 \rightarrow L_2$. It is again plausible that this $N = \infty$ transition (although not our estimate in eqn(16)) will survive as $L_3 \rightarrow L_2 \rightarrow L_1 \rightarrow L_0$, thus making the connection with the third transition observed on L^4 lattices [7, 8].

(3) If we increase β further we come to consider a field theory with a finite Euclidean time extent given by aL_3 living in an infinitesimal spatial volume $a^3 L_0 L_1 L_2$. Such systems can in

principle have deconfining phase transitions [26] although whether this one does or not we do not attempt to make plausible by a simple argument. If it does exist then it would provide the final step in our cascade of $N = \infty$ phase transitions $\beta_{c_0} \ll \beta_{c_1} \ll \beta_{c_2} \ll \beta_{c_3}$ on our $L_0 \ll L_1 \ll L_2 \ll L_3$ lattices.

The above discussion has taken the $D = 3 + 1$ $SU(N)$ gauge theory as its starting point. It is obvious that we could equally well have started with a $L_0 \ll L_1 \ll L_2$ $D = 2 + 1$ $SU(N)$ gauge theory and followed that through a cascade of deconfining $N = \infty$ transitions.

4 Results

4.1 Preliminaries

4.1.1 Phase transitions

At a phase transition appropriate derivatives of the partition function Z diverge or are discontinuous. (Strictly speaking of $\frac{1}{V} \log Z$ where V is the volume.) The lowest order of such a singular derivative determines the order of the phase transition. For Z or its derivatives to be singular, we require an infinite number of degrees of freedom, and this usually demands an infinite volume, with a cross-over at finite V sharpening to the appropriate singularity as $V \rightarrow \infty$. As $N \rightarrow \infty$ we have the possibility of a new kind of phase transition that takes place in a finite volume with the infinite number of degrees of freedom being provided by N .

With the standard plaquette action, a conventional first order transition has a discontinuity at $V = \infty$ in the average plaquette,

$$\langle u_p \rangle = N_p^{-1} \partial \log Z / \partial \beta \quad (17)$$

where N_p is the number of plaquettes. (We denote the space-time volume by V and note that $V = N_p/3$ in $D = 2 + 1$.) At finite V this discontinuity is a rapid crossover so that

$$\partial \langle u_p \rangle / \partial \beta = N_p^{-1} \partial^2 \log Z / \partial \beta^2 \equiv C \quad (18)$$

diverges at the critical coupling $\beta = \beta_c$ as $N_p \rightarrow \infty$. (Here C is the specific heat.) This divergence is linear in V since the cross-over between the two distinct values of the plaquette occurs in the range of $\beta - \beta_c$ where there is back-and-forth tunnelling and this range is $O(1/V)$ as we see from the linear approximation

$$\Delta F(\beta) = V \Delta f(\beta) \propto (\beta - \beta_c) V \sim O(1) \quad (19)$$

to the free energy (density) difference, $\Delta F, f$, between the two phases.

A conventional second order transition has a smooth first derivative of Z but a diverging second derivative and specific heat $C \rightarrow \infty$ as $V \rightarrow \infty$. Defining $\overline{u_p}$ to be the average value of u_p over the space-time volume for a single lattice field, we easily see that the specific heat can be written as a correlation function:

$$\begin{aligned} C &= N_p \langle (\overline{u_p} - \langle \overline{u_p} \rangle)^2 \rangle = N_p (\langle \overline{u_p}^2 \rangle - \langle \overline{u_p} \rangle^2) \\ &= \sum_p \langle (u_p - \langle u_p \rangle)(u_{p_0} - \langle u_p \rangle) \rangle \end{aligned} \quad (20)$$

where p_0 is some arbitrary reference plaquette. It is clear from eqn(20) that the divergence of C as $N_p \rightarrow \infty$ implies that there is a diverging correlation length – the standard signal of a second order phase transition.

A conventional third order transition has smooth first and second order derivatives but a singular third-order derivative, $C' \equiv N_p^{-1} \partial^3 \log Z / \partial \beta^3$, at $V = \infty$. This may be written as

$$\begin{aligned} C' &= \frac{\partial C}{\partial \beta} = N_p^2 \langle (\overline{u_p} - \langle \overline{u_p} \rangle)^3 \rangle \\ &= N_p^2 (\langle \overline{u_p}^3 \rangle - 3 \langle \overline{u_p} \rangle \langle \overline{u_p}^2 \rangle + 2 \langle \overline{u_p} \rangle^3). \end{aligned} \quad (21)$$

Note that if the fluctuations of $\overline{u_p}$ were symmetric around $\langle \overline{u_p} \rangle$, as they are for $\beta = 0$, then C' would be zero, so

$$\lim_{\beta \rightarrow 0} C'(\beta) = 0. \quad (22)$$

It should be clear that the higher the order of the transition, the greater is the statistics needed to determine its properties to a given precision. In particular, identifying third-order transitions is already a formidable numerical challenge, and we do not attempt to look for transitions that are of yet higher order.

Since we are particularly interested in transitions that develop as $N \rightarrow \infty$ and since we know that, in general, fluctuations in the pure gauge theory decrease by powers of N in the large- N limit [12, 27] it is convenient to define the rescaled quantities

$$C_2 = N^2 \times C \quad ; \quad C_3 = N^4 \times C' \quad (23)$$

which one expects generically to have finite non-zero limits when $N \rightarrow \infty$. (Note that the increasing power of N simply matches the increasing power of $\partial/\partial\beta = 2N^2\partial/\partial\gamma$, where γ is the inverse 't Hooft coupling defined in eqn(4).) The signature of a phase transition which is only present for $N = \infty$ will be a crossover for finite N at which fluctuations decrease more slowly than the naive power of $1/N^2$. If, therefore, we find a crossover in C_2 or C_3 which does not sharpen with increasing volume at fixed N , but rather becomes a divergence or a discontinuity only in the large- N limit, then this will indicate a second- or third-order $N = \infty$ phase transition respectively. (Provided of course that $\langle u_p \rangle$ is continuous so that there is no large- N first order transition.)

Large- N phase transitions can have an unconventional behaviour. Consider for example a second order transition characterised by a value of C_2 that diverges at some $\lambda = \lambda_c$ as $N \rightarrow \infty$. This may indeed be due to a correlation length ξ that diverges (in lattice units) as $N \rightarrow \infty$: $\xi(\lambda_c) \propto N^\alpha$; $\alpha > 0$. However there is another, less conventional, possibility: the correlation length may be finite and it may be that local plaquette fluctuations have an anomalous N -dependence at the critical point: $\langle u_p^2 \rangle / \langle u_p \rangle^2 - 1 \propto N^{\alpha-2}$; $\alpha > 0$.

Since large- N phase transition can arise from fluctuations that are completely local – as in $D = 1 + 1$ where the lattice partition function factorises – it is also useful to consider local versions of the quantities C_2 and C_3 :

$$P_2 = N^2 \times (\langle u_p^2 \rangle - \langle u_p \rangle^2) \quad (24)$$

and

$$P_3 = N^4 \times (\langle u_p^3 \rangle - 3\langle u_p \rangle \langle u_p^2 \rangle + 2\langle u_p \rangle^3). \quad (25)$$

These are the contributions to C_2 and C_3 from fluctuations of individual plaquettes, i.e. neglecting correlations between plaquettes. So calculations of P_2 and P_3 require much lower statistics than C_2 and C_3 to achieve the same accuracy, and this will be particularly useful at the largest values of N . Of course, divergences or discontinuities in P_2 or P_3 will normally imply divergences or discontinuities in C_2 or C_3 , even if the latter are not visible in the statistical noise of the numerical calculation. Note that in 1+1 dimensions, where the theory factorises and there are no propagating degrees of freedom, we have $P_2 = C_2$ and $P_3 = C_3$ at any N .

The eigenvalues of an $SU(N)$ matrix such as the plaquette, are gauge-invariant, and so we can use them to gain additional information to that encoded in the above correlators of low powers of traces of plaquettes. Indeed, at the $D = 1 + 1$ $N = \infty$ Gross-Witten transition a gap opens in the eigenvalue density of the plaquette [1]. That is to say, while in the strongly-coupled phase the eigenvalue density is non-zero for all angles $-\pi \leq \alpha \leq \pi$, in the weakly-coupled phase it is only non-zero in the range $-\alpha_c \leq \alpha \leq \alpha_c$, where $\alpha_c < \pi$. To search for a similar transition in 2+1 dimensions we will measure the total plaquette eigenvalue density. Using the eigenvalue density directly to search for a gap is difficult since for any finite N there is not a true gap but instead a (near-)exponential drop in the eigenvalue density as $\alpha \rightarrow \pm\pi$, so very good statistics are required to observe changes in the exponentially suppressed tails of the density. To avoid relying solely on the accurate calculation of these tails, we also calculate the fluctuations of the eigenvalues around their average values, $\langle \lambda_i^2 \rangle - \langle \lambda_i \rangle^2$, where λ_i is the i th eigenvalue when ordered by its phase. (Recall that the eigenvalues of $SU(N)$ matrices are pure phases $\lambda_j = \exp\{i\alpha_j\}$.) In particular, we shall calculate the normalised ratio for the extreme (smallest) eigenvalue:

$$R_p = \frac{\langle \lambda_1^2 \rangle - \langle \lambda_1 \rangle^2}{\langle \lambda_{\frac{N}{2}}^2 \rangle - \langle \lambda_{\frac{N}{2}} \rangle^2} \quad (26)$$

(for N even). This is motivated by the situation in the $N \rightarrow \infty$ limit in $D = 1 + 1$ where the eigenvalue density at the Gross-Witten transition, $\gamma = 1/2$, is [1] $\frac{1}{2\pi}(1 + \cos\alpha)$. This density approaches zero as $\alpha \rightarrow \pm\pi$ but is finite at $\alpha = 0$, so we expect the fluctuations to be $O(1/N)$ in $\lambda_{\frac{N}{2}}$ while they can be up to $O(1)$ for λ_1 . Thus we expect R_p to diverge at the Gross-Witten transition, and it may provide a useful observable in our search for a similar transition in $D = 2 + 1$.

4.1.2 Wilson loop non-analyticities

To investigate the possibility that Wilson loops undergo some analogous non-analyticity as their area passes through some critical value, A_{crit} , we calculate Wilson loops of a fixed size, $n_1 \times n_2$, in lattice units and increase β so as to decrease the lattice spacing a and hence the area, $A = an_1 \times an_2$, in physical units. If there is a non-analyticity at $A(\beta_c(n_1, n_2))$ we can then vary n_1, n_2 so as to check whether the transition occurs at a fixed area in the continuum

limit, when expressed in units of say $g^2 N$, i.e. whether

$$\frac{A_{crit}}{(g^2 N)^2} = \lim_{a \rightarrow 0} \left(\frac{\beta_c}{2N^2} \right)^2 A(\beta_c) \quad (27)$$

is finite and non-zero. Since all the evidence is that the $D = 2 + 1$ $SU(N)$ lattice gauge theory has no phase transition, at zero temperature, once λ is on the weak coupling side of the bulk transition, we expect any Wilson loop non-analyticity not to correspond to a phase transition of the whole system. This will be an important constraint on what are the important observables to calculate. We also expect that any such transitions will be cross-overs at finite N , becoming real non-analyticities only at $N = \infty$. This is because we can imagine that they are driven by the degrees of freedom close to the critical length scale, and that we need these to be infinite in number for a real non-analyticity.

We remarked in Section 3.2 that a non-analyticity in the eigenvalue spectrum of the Wilson loop is known to occur [9, 10] in the $D = 1 + 1$ $N = \infty$ gauge theory at the critical area given in eqn(7). We have performed numerical lattice calculations in this theory for large N and find that the lattice critical area is very close to the continuum one for Wilson loops that are 2×2 or larger. To be more precise let us denote the product of link matrices around a square $n \times n$ Wilson loop by $U_w^{n \times n}$ and its trace by $u_w^{n \times n} = \frac{1}{N} \text{ReTr}\{U_w^{n \times n}\}$ which we generically write as u_w . Then we find that the non-analyticity occurs when u_w reaches a particular value

$$\langle u_w \rangle \simeq e^{-2}. \quad (28)$$

As an example we show in Fig. 1 the eigenvalue spectrum of a 3×3 Wilson loop in $D = 1 + 1$ for $N = 48$ at $\lambda = 0.7971$ where the trace satisfies eqn(28) and we compare it to the continuum expression obtained from [9, 10]. We clearly have a very good match (apart from the $N = 48$ bumps that arise from the eigenvalue repulsion in the Haar measure). Now we know that in $D = 1 + 1$ the Wilson loop factorises into a product of plaquettes

$$\langle u_w \rangle = \langle u_p \rangle^{\frac{A}{a^2}} \quad (29)$$

and that $\langle u_p \rangle = 1 - \lambda/4$ at $N = \infty$ [1]. Putting all this together, we have

$$\left(1 - \frac{\lambda}{4} \right)^{\frac{A}{a^2}} = e^{\frac{A}{a^2} \ln(1 - \frac{\lambda}{4})} \xrightarrow{a \rightarrow 0} e^{-\frac{A\lambda}{4a^2}} \simeq e^{-2} \quad (30)$$

which we observe is nothing but the continuum relation in eqn(7). These numerical calculations show that lattice corrections are small except for loops smaller than 2×2 , such as the plaquette that has its non-analyticity at the Gross-Witten transition where $\lambda = 2$. Because of the factorisation in eqn(29) the trace of u_w will be analytic in the (bare) coupling when this gap in the eigenvalue spectrum forms (except for the very smallest loops where it occurs at the Gross-Witten transition) and so it is not immediately obvious what is the significance of this gap formation. What this tells us, nonetheless, is that we should not only search in $D = 2 + 1$ for non-analyticities of traces of Wilson loops, but also for such eigenvalue gap formation.

Our initial question will be whether $\langle u_w \rangle$ has a non-analyticity in λ for some value of the area, A/a^2 . To investigate this we can look at $\langle u_w \rangle$ and its derivatives as a function of the bare coupling λ . The derivatives can be expressed as correlation functions in the usual way e.g.

$$\begin{aligned} \partial \langle u_w \rangle / \partial \beta &= N_p (\langle u_w \overline{u_p} \rangle - \langle \overline{u_p} \rangle \langle u_w \rangle) \\ &= \sum_p \langle (u_w - \langle u_w \rangle)(u_p - \langle u_p \rangle) \rangle. \end{aligned} \quad (31)$$

Because the whole system has no phase transition we expect that the non-analyticity will be visible in the ‘local’ correlators analogous to those in eqns(24,25) e.g.

$$P_2^w = N^2 \times (\langle u_w \hat{u}_p \rangle - \langle u_w \rangle \langle \hat{u}_p \rangle) \quad (32)$$

where \hat{u}_p is the average of the plaquettes that tile the minimal Wilson loop surface. We define P_3^w in analogy to P_3 in the same way.

It is also possible that some non-analyticity might be present in just the fluctuations of Wilson loops rather than in the derivatives with respect to the coupling. Thus we also consider the correlators

$$W_2^{n \times n} = N^2 \times (\langle u_w^{n \times n^2} \rangle - \langle u_w^{n \times n} \rangle^2) \quad (33)$$

and

$$W_3^{n \times n} = N^4 \times (2\langle u_w^{n \times n} \rangle^3 - 3\langle u_w^{n \times n} \rangle \langle u_w^{n \times n^2} \rangle + \langle u_w^{n \times n^3} \rangle). \quad (34)$$

that represent an alternative generalisation to Wilson loops of the quantities P_2 and P_3 defined in eqns(24,25).

In searching for a gap formation in the eigenvalue spectrum of an $n \times n$ Wilson loop, we define the quantity $R^{n \times n}$ in direct analogy to the quantity R_p defined in eqn(26). However this quantity is only useful for the bulk transition because the eigenvalue spectrum approaches the gap with a finite slope. We know that for larger Wilson loops in $D = 1 + 1$ [9, 10] the approach is with a diverging slope (at $N = \infty$), and that $R^{n \times n}$ is not a useful observable in that case. We shall in fact find it much more useful to match the eigenvalue spectra in $D = 2 + 1$ and $D = 1 + 1$. That this is in fact possible is one of our most interesting results.

4.2 Bulk transition

In 3+1 dimensions the bulk transition is easily visible as a large discontinuity in the action for $N \geq 5$ (where the transition is first order) and as a (finite) peak in the specific heat for $N \leq 4$ (where the transition is a crossover). We have searched for an analogous jump or rapid crossover in 2+1 dimensions, in particular around $\gamma \equiv \beta/2N^2 \sim 1/2$.

In Fig.2 we display the values of the average plaquette for $SU(6)$, $SU(12)$, $SU(24)$ and $SU(48)$ as obtained on 6^3 lattices. At $\gamma \sim 1/2$ an $L = 6$ lattice has a size $La\sqrt{\sigma} \sim 3$ and so is large enough that it should display a very sharp cross-over for a conventional first-order transition. This should be more so as $N \uparrow$ and (most) finite volume effects disappear. As a check we have repeated our calculations on 12^3 lattices for $SU(6)$ and have found no volume

dependence. What we see in Fig. 2 is that the action appears to be approaching a smooth crossover in the large- N limit, with no evidence for a first order phase transition either at finite N or at $N = \infty$.

Our results for the specific heat C_2 for $SU(6)$ and $SU(12)$ are shown in Fig. 3. (For $SU(24)$ and $SU(48)$ our accuracy is insufficient to get useful results for C_2 .) There is a clear peak around $\gamma \simeq 0.42$ which appears to be growing stronger with increasing N . For $SU(6)$ we repeated our calculations on 12^3 lattices and found no volume dependence. This tells us that we are not seeing a conventional second-order phase transition at fixed N for which the specific heat peak grows as the volume increases (since a larger volume can better accommodate the diverging correlation length). So if there is a second-order phase transition here it would appear to be not at finite N , but only at $N = \infty$.

To search for a possible third order transition we calculate C_3 , but our calculations are not accurate enough to produce anything significant, even for $SU(6)$.

To improve our reach in N we calculate the quantities P_2 and P_3 defined in eqns(24,25). These represent the contributions to C_2 and C_3 made by the fluctuations of individual plaquettes and are the quantities that reveal the Gross-Witten transition in $D = 1 + 1$. In Fig. 4 we show the values of P_2 obtained for $SU(6)$, $SU(12)$, $SU(24)$ and $SU(48)$. We observe, as expected, a dramatic reduction in the statistical errors as compared to C_2 in Fig. 3, enabling us to look for fine structure in the β -dependence. There is no significant evidence for a peak in P_2 which indicates that if there is a second order transition at $N = \infty$, as suggested by the peak in C_2 , it will primarily involve correlations between different plaquettes rather than arising from the fluctuations of individual plaquettes. What we do see in P_2 however is definite evidence for a cusp developing with increasing N , at $\gamma \simeq 0.43$, where the derivative of P_2 will suffer a discontinuity. This corresponds to a third-order transition at $N = \infty$, just like the $D = 1 + 1$ Gross-Witten transition [1]. It is therefore useful to compare the $D = 1 + 1$ and $D = 2 + 1$ cases in more detail. For this purpose we show in Fig. 5 some numerically calculated values of P_2 in $D = 1 + 1$ $SU(6)$, $SU(12)$ and $SU(24)$ gauge theories. (Recall that in $D = 1 + 1$ the factorisation of the partition function implies that $C_2 = P_2$.) We also plot the analytic results for $SU(\infty)$ [1]:

$$P_2 = C_2 = \begin{cases} \frac{1}{2}, & \gamma \leq 0.5 \\ \frac{1}{8\gamma^2}, & \gamma \geq 0.5. \end{cases} \quad (35)$$

Apart from a small relative shift in γ the results for $D = 2 + 1$ and $D = 1 + 1$ are remarkably similar, strengthening the evidence for a third-order $N = \infty$ transition.

To investigate this further, we show in Fig. 6 our results for P_3 for $SU(6)$, $SU(12)$, $SU(24)$ and $SU(48)$. There is clearly an increasingly sharp transition as N increases around $\gamma \simeq 0.43$. For comparison we show in Fig. 7 corresponding numerical results for $D = 1 + 1$ (where $C_3 = P_3$) together with the analytic result for $SU(\infty)$ [1]:

$$C_3 = \begin{cases} 0, & \gamma \leq 0.5 \\ -\frac{1}{8\gamma^3}, & \gamma \geq 0.5. \end{cases} \quad (36)$$

which has a discontinuity at the Gross-Witten transition at $\gamma = 1/2$. It is clear that once again the the behaviour in $D = 2 + 1$ is remarkably similar to that in $1+1$ dimensions.

We see further evidence for a Gross–Witten–like transition in our results for the ratio R_p defined in eq. 26. Our results for $SU(6)$, $SU(12)$, $SU(24)$ and $SU(48)$ are plotted in Fig. 8. There is a clear peak around $\gamma \simeq 0.43$ whose height increases rapidly with N , indicating that the fluctuations of the extreme eigenvalues are becoming much larger than fluctuations of the ‘middle’ eigenvalue (the one nearest $\alpha = 0$). Very similar behaviour occurs in 1+1 dimensions, for which our results are shown in Fig. 9. Indeed, in the $N \rightarrow \infty$ limit in 1+1 dimensions we expect that R_p will diverge, as discussed below eq. 26. This appears to be exactly what we see in Fig. 9.

Finally we compare the $D = 2 + 1$ and $D = 1 + 1$ transitions directly by comparing the eigenvalue densities across the transition. We do this for $SU(12)$ in Fig. 10. The eigenvalue densities both below and above the transition are clearly very similar in 1+1 and 2+1 dimensions.

All the above confirms that $D = 2 + 1$ $SU(N)$ gauge theories possess an $N = \infty$ third-order strong-to-weak coupling transition that is remarkably similar, even in its details, to the $D = 1 + 1$ Gross–Witten transition.

Despite this striking similarity, when we look in more detail we also observe significant differences between the bulk transition in 2+1 dimensions and the Gross–Witten transition. Comparing Figs. 3 and 5, we see that there is a peak in the specific heat in $D = 2 + 1$ which is simply not present in $D = 1 + 1$. From Fig. 4 it is clear that this peak does not come from fluctuations of individual plaquettes, but must come from correlations between different plaquettes. To investigate this we consider the following particular contributions to the specific heat C_2 : the contribution from correlations between a plaquette and its neighbours in the same plane, which we label C_i ; the contribution from correlations between a plaquette and its neighbours which share an edge but are not in the same plane, C_o ; and finally C_f , the contribution from correlations between a plaquette and the plaquettes facing it across an elementary cube. We include a factor N^2 , as for C_2 . We find a clear peak, growing with N , in our results for C_o , plotted in Fig. 11. The peak accounts for about half of the difference between C_2 and P_2 . There is also a much weaker peak in C_i , approximately a factor of 15 times smaller, which also clearly grows with N , at least up to $N = 24$. (The weakness of the signal means that we lose statistical significance for larger N .) For C_f , where we happen to have results only for $SU(6)$ and $SU(12)$, we see in both cases a clear peak. This is almost exactly a factor of four lower than the corresponding peak for C_o . Since each plaquette has four times as many out-of-plane neighbours as it has neighbours facing it across an elementary cube, this shows the correlation of a plaquette with its individual out-of-plane neighbours is in fact the same as with a facing plaquette. By contrast the correlation with the ‘nearer’ neighbouring plaquettes that are in the same plane (as measured by C_i) is very much weaker. This pattern is precisely what one would expect if the correlations were due to a flux emerging from the cube symmetrically through every face, i.e. due to the presence of monopole–instantons.

If such monopoles are present, we would expect the correlation of the plaquette with itself, P_2 , to be also affected. These correlations of the plaquette with itself should be as large as with each of its eight out-of-plane neighbours, so this contribution to P_2 should be about one eighth of C_o . Even for $SU(48)$ this is only ~ 0.04 , which is easily consistent with our results in Fig. 4. Of course, if there really is a second-order phase transition at $N = \infty$, then eventually

we would expect to see a growing peak in P_2 . It is of course possible that there is no second-order phase transition at $N = \infty$, but only a rapid cross-over, so that C_o asymptotes to a finite value, and in that case there would not need be a pronounced peak in P_2 . This however seems a rather artificial scenario.

Since a second-order transition is usually associated with a diverging correlation length, we also measured the mass of the lightest particle that couples to the plaquette, in both $SU(6)$ and $SU(12)$. We calculate an effective mass at a separation of n lattice units:

$$am_{\text{eff}}(n) = -\ln \frac{\langle \phi_0 \phi_n \rangle - \langle \phi_0 \rangle^2}{\langle \phi_0 \phi_{n-1} \rangle - \langle \phi_0 \rangle^2} \quad (37)$$

where ϕ_0 is the trace of a plaquette and ϕ_n is the trace of a facing plaquette lying in the same plane n lattice spacings away. This is not a zero-momentum correlator, so it will overestimate the masses. (We do not have a statistically significant signal from zero-momentum correlators.) Our results for $am_{\text{eff}}(1)$ are plotted in Fig. 12. (Our results for $n \geq 2$ do not have a useful statistical accuracy.) We observe a dip in the effective masses near the transition, which becomes more significant for $SU(12)$, particularly when we take into account the expected weak-coupling scaling behaviour, $am \propto 1/\beta$. While this is certainly consistent with a second-order cross-over, the masses are large, and if the correlation length is going to show any sign of diverging it is clear that it will be at a much larger value of N than are accessible to our calculations.

4.3 Wilson loops

4.3.1 Traces and correlators

In Fig 13 we show how $\langle u_w \rangle$ varies with λ in some sample calculations. We see no sign of any singularity developing in this quantity, or in our simultaneous calculations of $\partial \langle u_w \rangle / \partial \lambda$, in contrast to the growing peak we saw for $C_2 \propto \partial \langle u_w \rangle / \partial \lambda$ in Fig. 3. The local version of the correlator corresponding to the first derivative defined in eqn(32), P_2^w , is more accurately calculated and its variation with λ is shown in Fig 14 and shows no evidence of a developing cusp that would suggest an $N = \infty$ singularity in the second derivative. Thus, at this level of accuracy, we see no evidence for any $N = \infty$ non-analyticity in the variation of $\langle u_w \rangle$ as a function of the coupling λ .

Given our uncertainty in the type of analyticity that might occur we have also considered it worthwhile to look at the quantities $W_2^{n \times n}$ and $W_3^{n \times n}$ which are defined in eqs. 33 and 34 and which are alternative analogues of the quantities P_2 and P_3 for the plaquette. Some results for $SU(6)$, $SU(12)$, $SU(24)$ and $SU(48)$ are plotted in Fig. 15. While there is a range of $\gamma = 1/\lambda$ over which $W_2^{2 \times 2}$ stops being constant and starts to decline, this ‘transition’ does not become sharper with N , in contrast to the behaviour of the plaquette equivalent, P_2 , in Fig. 4. We see the same behaviour for 3×3 and 4×4 Wilson loops, only shifted to higher γ , with no sign of the transitions becoming sharper as N increases. Our results for $W_3^{2 \times 2}$ for $SU(6)$ and $SU(12)$ are plotted in Fig. 16. While there is a transition region in which $W_3^{2 \times 2}$ becomes negative, just as one sees for P_3 in Fig. 6, the transition does not become sharper as

N increases, unlike P_3 . Again we see the same behaviour for $W_3^{3 \times 3}$ and $W_3^{4 \times 4}$, with no sign of the transitions becoming sharper as N increases.

All these results are in fact essentially identical to those we obtain in similar calculations in $D = 1 + 1$, where we know that the $\langle u_w \rangle$ is analytic in λ except at the Gross-Witten transition.

Finally we recall that for the plaquette the Gross-Witten transition is characterised by a divergence in the relative fluctuation of extremal eigenvalues, as shown in Fig. 8. For $n \times n$ Wilson loops the analogous quantity, $R^{n \times n}$, shows no such behaviour, as we see, for the example of $R^{2 \times 2}$ for $SU(6)$, $SU(12)$ and $SU(24)$ plotted in Fig. 17. This is perhaps no surprise, given that in $D = 1 + 1$ the eigenvalue gap formation for Wilson loops larger than the plaquette does not involve growing fluctuations of the extremal eigenvalues.

4.3.2 Matching eigenvalue spectra

Although we have found no evidence that the trace of a Wilson loop is non-analytic in λ at some critical area, it is possible that there are more subtle non-analyticities of the kind that exist in $D = 1 + 1$ and which are associated with a gap forming in the eigenvalue spectrum.

To determine numerically whether at some given λ the spectrum $\rho(\alpha)$ in some region close to $\alpha = \pm\pi$ will extrapolate exactly to zero when $N \rightarrow \infty$ is clearly a delicate matter, given that the values at finite N from which we extrapolate are already extremely small.

So to search for such non-analytic behaviour we explore the strategy of directly comparing Wilson loop eigenvalue spectra in 1+1 and 2+1 dimensions. We first evaluate the spectrum in 1+1 dimensions at the critical coupling at which the gap forms. A true gap only forms at $N = \infty$; for finite N we use the same value of the critical 't Hooft coupling, [9, 10]

$$\lambda_c = \frac{1}{\gamma_c} = 4(1 - e^{-\frac{2a^2}{A}}), \quad (38)$$

where A is the area of the Wilson loop in physical units. At this coupling the expectation value of the trace of the Wilson loop is, using eqn(6) [9, 10],

$$\langle u_w \rangle = \{\langle u_p \rangle\}^{A/a^2} \stackrel{N \rightarrow \infty}{=} \left(1 - \frac{\lambda}{4}\right)^{A/a^2} = e^{-2}, \quad (39)$$

which is the same value as at the critical coupling in the continuum limit. Note also that as $a \rightarrow 0$ and $A/a^2 \rightarrow \infty$, eqn(38) reduces to eqn(7) as it should. Having obtained the spectrum (numerically) in $D = 1 + 1$ for a given size Wilson loop (in lattice units) and for a given value of N , we then calculate the eigenvalue spectrum in $D = 2 + 1$ for the same size loop and for the same N , varying the coupling to a value where the two eigenvalue spectra match.

We find that it is always possible to achieve such a match, for any N and for any size of Wilson loop. We show an example in Fig. 18, where we compare the eigenvalue density of the 3×3 Wilson loop in $SU(12)$ in 1+1 dimensions to the density in 2+1 dimensions, at a coupling chosen to give the best match. In Fig. 18 the coupling in $D = 1 + 1$ is λ_c , the coupling at which the gap forms. The spectra are clearly very similar and indeed indistinguishable on this plot. We also find that the spectra can be matched when they are away from the critical coupling:

we show this in Fig. 19, where we choose a higher value of γ to illustrate that the matching continues to work after the gap forms. In Figs. 18 and 19 we also plot the analytically known spectra [9, 10]. in the continuum limit of the $N = \infty$ theory in $D = 1 + 1$ at the corresponding couplings. These clearly match the corresponding finite- N spectra very well, except in two respects: the latter have N bumps which arise from the eigenvalue repulsion that is a well-known characteristic of the Haar measure, and the finite- N spectrum is not precisely zero in the region of the ‘gap’.

The fact that at finite but large N we can match so precisely the $D = 1 + 1$ and $D = 2 + 1$ eigenvalue spectra for couplings at and above the $D = 1 + 1$ transition, provides convincing evidence that the Wilson loops in the $D = 2 + 1$ $N = \infty$ theory also undergo a transition involving the formation of a gap in the eigenvalue spectrum.

In Fig. 20 we plot the eigenvalue spectra of 2×2 , 3×3 , and 4×4 loops in $SU(6)$ in $2+1$ dimensions. The three couplings have been chosen so as to give the best match to the eigenvalue spectra of Wilson loops of the same size in $D = 1 + 1$ at λ_c . We see that the three spectra are essentially identical. Moreover the critical value of the $D = 2 + 1$ coupling $\gamma_c = 1/\lambda_c$ appears to grow linearly with the size of the $L \times L$ loop, suggesting that there is a finite critical area for gap formation in the continuum limit: [9, 10]

$$\lambda_c^2 L^2 \stackrel{a \rightarrow 0}{=} (ag^2 N)^2 L^2 = (g^2 N)^2 A_{crit}. \quad (40)$$

As we shall see below, in Section 4.3.4, this is nearly but not quite the case.

It turns out that all the above is an immediate corollary of a much stronger and rather surprising result concerning the matching of Wilson loop eigenvalue spectra in $1+1$ and $2+1$ (and indeed $3+1$) dimensions.

The general statement is that if take an $n \times n$ Wilson loop $U_w^{n \times n}$ in the $SU(N)$ gauge theory and calculate the eigenvalue spectra in D and D' dimensions, we find that the eigenvalue spectra match at the couplings λ_D and $\lambda_{D'}$ at which the averages of the traces $u_w^{n \times n} = \frac{1}{N} \text{ReTr}\{U_w^{n \times n}\}$ are equal:

$$\langle u_w^{n \times n}(\lambda_D) \rangle_D = \langle u_w^{n \times n}(\lambda_{D'}) \rangle_{D'}. \quad (41)$$

We have tested this matching for $D = 1 + 1$ and $D = 2 + 1$ over groups in the range $N = 2$ to $N = 48$ and for Wilson loops ranging in size from 1×1 (the plaquette) to 8×8 and, in $2+1$ dimensional, for couplings from $\lambda = 4.0$ to $\lambda = 0.40$. We have in addition tested it in the deconfined as well as in the confined phase. Some sample calculations in $D = 3 + 1$ have also been performed [15] strongly suggesting that the same is true there.

The fact that such a precise matching is possible implies that the eigenvalue spectrum is completely determined by N , the size of the loop, and its trace. Hence the eigenvalues are not really independent degrees of freedom, which is unexpected. Moreover we have seen in Fig. 20 a demonstration of the fact that the spectra of Wilson loops that are 2 and larger can also be matched with each other. The matching occurs at values of the traces that are the same as those in $D = 1 + 1$ where they are calculable. In this sense, the size of the Wilson loop is not really an extra variable here. Finally, the N dependence is weak, and consists mainly of the two differences noted earlier.

Finally we remark that our results at this stage rely on a comparison that is visual and impressionistic. Ideally one would like to match the spectra by varying λ continuously and this can be done, from nearby calculated values of the coupling, by standard reweighting techniques. In addition it would be useful to quantify any differences (which must be very small) with a standard error analysis. We intend to provide such analyses elsewhere [15].

4.3.3 Polyakov loops

We have also investigated the eigenvalue spectra of Polyakov loops as defined in Section 2. These are products of link matrices that wrap around one of the space-time tori (and are of minimal length unless specified otherwise) i.e. they can be thought of as non-contractible Wilson loops. They provide the conventional order parameter for the deconfinement phase transition. As one crosses this transition the Polyakov loop that winds around the time (temperature) torus acquires a non-zero expectation value. This corresponds to the spontaneous breaking of a global centre symmetry in the Euclidean system. To simulate the system at temperature T we use a $L_s^2 L_0$ lattice with $L_s \gg L_t$ so that $T = 1/aL_0$. As N grows one can weaken the inequality, so that one can take $L_s \rightarrow L_t$ as $N \rightarrow \infty$ while still maintaining the thermodynamic interpretation and the sharp phase transition.

We calculated the eigenvalue spectra of timelike Polyakov loops in $SU(12)$ on $L_s^2 L_0$ lattices. We found that it is always possible to match the Polyakov loop eigenvalue spectra to those of Wilson loops in 1+1 dimensions (and hence also to Wilson loops in 2+1 dimensions) by choosing couplings at which the trace of the Polyakov loop equals that of the Wilson loop

$$|\langle \bar{l}_{\mu=0} \rangle| = \langle u_w \rangle \quad (42)$$

where, as we have seen, the size of the Wilson loop does not matter to a very good approximation. (We take the modulus because the Polyakov loop is proportional to some element of the centre in the deconfined phase and the modulus effectively rotates that element to unity. The eigenvalue spectrum also needs to be rotated by the same centre element.) This matching has the corollary that the Polyakov loop eigenvalue spectrum will develop a gap at $N = \infty$ when its trace crosses the critical value $|\langle \bar{l}_{\mu=0} \rangle| = e^{-2}$. For $N > 4$ the deconfining transition at $T = T_c$ is strongly first order and the value of $|\langle \bar{l}_{\mu=0} \rangle|$ will jump from $|\langle \bar{l}_{\mu=0} \rangle| = 0$ at $T < T_c$ to some non-zero value for $T = T_c^+$. The latter value will typically be greater than e^{-2} for small L_0 , i.e. for coarse lattice spacings, and will $\rightarrow 0$ as $a \rightarrow 0$ and hence $L_0 \rightarrow \infty$. Moreover for fixed L_0 the trace increases with increasing T . (See Section 4.3.4 for why this is so.) Thus for coarse lattice spacings we expect the gap formation to occur at the phase transition, $T = T_c$, while for larger L_0 it will not coincide with the deconfining transition; instead it will occur at some $T > T_c$. The critical value turns out to be $L_0 = 7$. Thus in the continuum limit the gap formation in timelike Polyakov loops does not occur at $T = T_c$ but rather at $T = \infty$.

As a numerical example of the eigenvalue matching we show in Fig 22, the eigenvalue spectra of the timelike Polyakov loop just below and just above the deconfinement transition for $L_t = 4$, together with a 3×3 Wilson loop spectrum in 1+1 dimensions at a coupling chosen to match the spectrum of the deconfined Polyakov loop. The spectra clearly match closely. Since the 1+1 dimensional γ is above γ_c for the 3×3 loop, the Wilson loop will develop a gap

at this coupling in the large- N limit. Hence the Polyakov loop will presumably also develop a gap.

Finally we recall that as $N \rightarrow \infty$ the deconfining transition occurs on smaller spatial volumes $L_s \rightarrow L_0$ so that at $N = \infty$ one can discuss the transition on a L^3 lattice. Taking into account the fact that our preliminary results [15] indicate that all the above carries over to Wilson and Polyakov loops in $D = 3 + 1$, we can make direct contact with the observation in [7, 8] that on an L^4 lattice the Polyakov loop develops a gap when it develops a non-zero expectation value.

4.3.4 Theoretical interpretation

The fact that at $N = \infty$ there is a gap at weak coupling in the eigenvalue spectra of Wilson loops, has a simple explanation in the theory of Random Matrices. (See e.g. [28] for a recent review.) At $N = \infty$ the Gaussian Unitary Ensemble (GUE) of complex Hermitian $N \times N$ matrices generates an eigenvalue spectrum that is the well-known Wigner semicircle

$$\rho(\lambda) \stackrel{N \rightarrow \infty}{\propto} \left(1 - \frac{\lambda^2}{4}\right)^{\frac{1}{2}}. \quad (43)$$

In weak coupling, when $\beta \rightarrow \infty$, the $SU(N)$ link matrices can be expanded in terms of the Hermitian gauge potentials and it is very plausible that the averages involved in the calculation of Wilson loops fall into the same ‘universality class’ as the GUE. That is to say, once the eigenvalues of Wilson loops are clustered close to unity, the fact that the phases are on a circle rather than on the line becomes irrelevant and the phases (suitably rescaled by the coupling) should be distributed according to the semi-circle in eqn(43). In fact this is precisely what we find. Thus the existence of a gap in the eigenvalue spectrum at weak coupling has a rather general origin in terms of Random Matrix Theory.

On the other hand we know that in a confining theory

$$\langle u_w \rangle \propto e^{-\sigma A} \xrightarrow{A \rightarrow \infty} 0 \quad (44)$$

which requires a nearly flat eigenvalue spectrum in $[-\pi, +\pi]$. Thus as we decrease the lattice spacing, the eigenvalue spectrum of a $L \times L$ Wilson loop must change from being nearly uniform to eventually having a Wigner semicircle gap. Thus at some bare coupling it must pass through a transition where the gap forms.

For this gap to be physically significant, it must occur at a fixed physical area in the continuum limit. However, as we shall now see, this is not the case for either $2 + 1$ or $3 + 1$ dimensions (in contrast to $D = 1 + 1$). The reason is the perturbative self-energy of the sources whose propagators are the straight-line sections of the Wilson loop. (Often referred to as the ‘perimeter term’.) The leading correction is given by the Coulomb potential $V_c(r)$ at the ‘cutoff’ $r = a$. For a Wilson loop whose size is $l \times l = aL \times aL$ in physical units, this correction is

$$\delta \log \langle u_w \rangle \propto l V_c(a) \propto \begin{cases} \lambda L \log a & D = 2 + 1 \\ \lambda L & D = 3 + 1 \end{cases} \quad (45)$$

using the fact that $V_c(r) \propto g^2 N \log r, g^2 N/r$ and $\lambda = ag^2 N, g^2 N$ in $D = 2+1, 3+1$ respectively. Let us, for illustrative purposes, assume that the full potential is given by this self-energy and the area piece, $\sigma A = a^2 \sigma L^2$, that comes from linear confinement. Then we have

$$\langle u_w \rangle \propto \exp \{ c\lambda L \log \lambda - c' \lambda^2 L^2 \} \quad : \quad D = 2 + 1 \quad (46)$$

using the fact that $a^2 \sigma \propto (ag^2 N)^2 = \lambda^2$ and $\log a = \log \lambda + \dots$ in $D = 2 + 1$, and

$$\langle u_w \rangle \propto \exp \left\{ c\lambda L - c' e^{-\frac{c}{\lambda}} L^2 \right\} \quad : \quad D = 3 + 1 \quad (47)$$

using the fact that $a^2 \sigma \propto \exp \{ -c_r/g^2 N \}$ in $D = 3 + 1$, where c_r is given by the coefficients of the 2-loop renormalisation group equation.

Consider first the $D = 2 + 1$ case in eqn(46). Since $\lambda L = ag^2 NL = g^2 Nl$ is the length scale in physical units, we see that if it were not for the weakly varying $\log \lambda$ term in eqn(46), the Wilson loop trace would be the same on the lattice and in the continuum (up to the usual $O(a^2)$ lattice corrections). That is to say, we expect that as we approach the continuum limit, $\lambda \rightarrow 0$, the critical area for gap formation will vanish

$$A_{crit} \propto \frac{1}{(\log \lambda)^2} \xrightarrow{a \rightarrow 0} 0 \quad (48)$$

rather than tending to some finite limit. At coarse a the logarithmic correction will be weak and one might well be tempted to perform an extrapolation to the continuum limit that does not include it. We illustrate all this with a numerical calculation of the coupling, and hence lattice spacing, at which $L \times L$ loops develop a gap. We define the appearance of a ‘gap’ in our finite- N calculations as the coupling at which the spectrum is closest to the spectrum of the $L \times L$ loop in 1+1 dimensions at the coupling γ_c , for the same N . For SU(2) we calculated this coupling for L up to 8 on 16^3 lattices. For SU(6) we calculated up to $L = 4$ on 6^3 lattices. We show our results in Fig. 21, together with a best fit to the SU(2) data which has the asymptotic behaviour in eqn(48). The numerical data shows deviations from linearity which could either be interpreted as low L corrections to an asymptotic scaling behaviour $\gamma = \lambda^{-1} \propto L$, or as a logarithmic violation of this asymptotic scaling. From our above analysis we know the latter to be the correct interpretation.

In contrast to the anomalous behaviour we see when taking the continuum limit of $\lambda_c(A)$, the large- N limit is achieved rapidly and smoothly. To illustrate this we list in Table 1 the coupling for which the 3×3 loop develops a gap for $N \in [2, 48]$. The critical coupling is essentially constant from SU(6) onwards, showing that we are in the large- N limit. Indeed, even for SU(2) the corrections are small.

In the case of $D = 3 + 1$ the self-energy diverges linearly and will normally dominate the trace for all λ in the weak coupling region. Thus we expect $A_{crit} \propto a^2$ up to logarithmic corrections from the running coupling, so that the gap formation occurs in the deep ultraviolet as we approach the continuum limit.

In contrast, in $D = 1 + 1$ where the Coulomb potential is linear $V_c(r) \propto g^2 Nr$, the self-energy term contributes at most a mere lattice spacing correction that vanishes in the continuum limit.

From the above discussion we see that the anomalous behaviour of A_{crit} as $a \rightarrow 0$ arises from divergent self-energy contributions. If the source had a finite mass, so that the propagator was smeared over some range $\delta r \sim 1/\mu$, we would evaluate the Coulomb self-interaction at $r = 1/\mu$ rather than at $r = a$ and hence would replace $\lambda L \log \lambda \rightarrow \lambda L \log \mu$ in eqn(46), and $\lambda L \rightarrow \lambda/\mu$ in eqn(47). Assuming the universality of the gap formation persists for such loops, we would then expect them to form a gap at a value of A_{crit} that is finite in the continuum limit if we have chosen μ to be finite in physical units. The value of A_{crit} will of course depend on the value of μ .

Similar considerations apply to Polyakov loops.

While the above considerations make plausible the universality aspect of the gap formation in Wilson and Polyakov loops, they do not explain our most striking result which is that the complete eigenvalue spectra can be matched across space-time dimension and loop size by merely matching traces.

Finally, whether the gap formation, and the associated non-analyticity, has any significant physical implications is unclear. For that to be so one would require that the gap should form at a fixed physical area A_{crit} in the continuum limit. As we have seen that is not the case in $D = 2 + 1$ or in $D = 3 + 1$ and is only the case in $D = 1 + 1$, where there are no propagating degrees of freedom and so no ‘physics’ in the usual sense. One can imagine regularising the divergent self-energies so that A_{crit} is finite and non-zero in the continuum limit, but then it would appear to depend on the regularisation mass scale μ used.

4.4 Finite volume

In Section 3.4 we argued that $D = 3 + 1$ $SU(N)$ gauge theories on $L_0 \ll L_1 \ll L_2 \ll L_3$ lattices undergo a series of $N = \infty$ phase transitions at $\beta_{c_0} \ll \beta_{c_1} \ll \beta_{c_2} \ll \beta_{c_3}$. These phase transitions are essentially deconfining transitions, $a(\beta_{c_i})L_i = 1/T_c^{D=4-i}$, in a dimensionally reduced theory. We argued that continuity, and vanishing finite size corrections at large N , link these transitions to the $N = \infty$ phase transitions on L^4 lattices discussed in [2, 8, 7].

The same argument clearly holds for $SU(N)$ gauge theories on $L_0 \ll L_1 \ll L_2$ lattices in $D = 2 + 1$. Here we provide some (very) exploratory numerical results in support of this scenario. We do so on lattices with a less than asymptotic ordering, $L_0 < L_1 < L_2$.

4.4.1 First transition

The first transition is the usual deconfining phase transition when $L_1, L_2 \rightarrow \infty$. It is second order for $SU(2)$ and $SU(3)$, either second or first order for $SU(4)$, and first order for $N \geq 5$ [24]. Because the latent heat for $N \geq 5$ is $\propto N^2$, the cross-over on a finite $L_0 < L_1, L_2$ lattice will become a first-order phase transition at $N = \infty$. All this is well-established and does not require further numerical confirmation in this paper.

4.4.2 Second transition

To search for the second transition we simulate $SU(12)$ gauge fields on a $L_0 L_1 L_2 = 2 \times 4 \times 40$ lattice over a large range of $\gamma = \beta/2N^2$. We calculate the Polyakov loop around the $\mu = 1$ torus, average it over the given lattice field, and take the modulus: $|\bar{l}_1|$. This provides the conventional order parameter for a deconfining transition with the $L_1 = 4$ torus providing the (inverse) temperature. We plot results for the average of this, $\langle |\bar{l}_{\mu=1}| \rangle$, at each value of γ in Fig. 23. We also plot values of the plaquette difference, $\langle (u_{01} - u_{02}) \rangle$, which should also reflect such a transition. We see in Fig. 23 a very clear signal for a transition at $\gamma \sim 3.2$ in both quantities. This occurs at a temperature $T_{c_1} \equiv T_c^{D=1+1} = 1/4a(\gamma \sim 3.2)$ in the reduced theory. In units of the usual deconfining temperature of the $D = 2 + 1$ gauge theory, $T_{c_0} = T_c^{D=2+1}$, this amounts to $T_{c_1} \sim 3T_{c_0}$.

The rapid, steep crossover suggests that the transition is first order. We find support for this when we plot a histogram of the values of $|\bar{l}_1|$ at some of the values of γ in the cross-over region. This is illustrated in Fig. 24 for an ensemble of $SU(12)$ fields on a $2 \times 4 \times 80$ lattice at $\gamma = 3.368$. We see a clear two state signal, with the peak at small $|\bar{l}_1|$ being naturally interpreted as coming from fields in the confining phase and the peak at large $|\bar{l}_1|$ as coming from fields in the deconfined phase. Such a two-state signal is typical of a first order deconfining transition.

The next question is whether this cross-over will sharpen into an actual phase transition in the two interesting limits: when we increase the spatial volume (here just aL_2) at fixed N ; or when we increase N at fixed volume. In addressing the former question we need to remark upon some special features of first-order transitions in the effective $D = 1 + 1$ theory that we are discussing here. The high temperature deconfined phase is normally characterised by a centre symmetry breaking so that $\bar{l} \sim c(\beta) \exp\{i2\pi n/N\}$ where $c(\beta)$ is a self-energy renormalisation factor. Two such phases, characterised by n and n' say, can coexist and will be separated by a domain wall whose tension we expect [29] to be

$$\sigma_k \propto k(N - k) \frac{T^2}{\sqrt{g_2^2 N}} \quad ; \quad k = |n - n'|, \quad T = \frac{1}{aL_1}. \quad (49)$$

In one spatial dimension the domain wall is just a ‘point’ and so the usual energy/entropy arguments tell us that at $T = 1/aL_1 \geq T_{c_1}$ the field will break up into domains of typical size

$$\Delta r \propto \exp \left\{ + \frac{\sigma_k}{T} \right\} \quad (50)$$

Thus at any T if we take $L_2 \rightarrow \infty$ the volume will consist of a ‘gas’ of domain ‘walls’, and hence domains, and on the average these will be equally distributed amongst all the centre phases, so that $\langle |\bar{l}_{\mu=1}| \rangle \rightarrow 0$. However on volumes that satisfy $L_1 \ll L_2 \ll \Delta r$ we will typically be in one domain and will thus have the usual deconfining signal of a non-zero value for $|\bar{l}_{\mu=1}|$. In addition it is clear that the lightest mass, m_p , coupling to the $\mu = 1$ Polyakov loop will not vanish at $T > T_{c_1}$ but will approximately satisfy $m_p \propto \exp\{-cNT/\sqrt{\lambda}\}$. Note that this mass decreases with increasing $L_1 = 1/aT_1$ in contrast to the stringy behaviour, $m_p \propto L_1$, in

the confining phase. It is clear from the above that our conventional signals for being in a deconfined phase become more complicated to interpret in $D = 1 + 1$.

Similar considerations apply to the deconfining transition itself. Suppose that there are confining and deconfining phases that differ by a free energy density f . At $T = T_{c_1}$ we have $f = 0$ so that the typical field will consist of a ‘gas’ of domain walls of typical size $\Delta r \propto \exp\{+\sigma_{cd}/T\}$ where σ_{cd} is the free energy of the confining-deconfining interface. This is the essential difference with higher dimensions. For large enough volume ($= L_2$) half the domains will be confining and half will be deconfining. Let us now increase the temperature T a little above T_{c_1} . Then $f = \epsilon_0(T - T_{c_1})$ near T_{c_1} , where $\epsilon_0 = [m]^0$ in $D = 1 + 1$. If $T - T_{c_1}$ is small enough, then $\Delta r f(T)/T \ll 1$ and the fraction of the volume that is still in the confined phase will be $\propto \exp\{-\Delta r f(T)/T\} \sim O(1)$. That is to say, the transition will take place over a range of temperatures ΔT that is no smaller than

$$\frac{\Delta T}{T_{c_1}} \propto \epsilon_0^{-1} \exp\{-\sigma_{cd}/T_{c_1}\} \quad (51)$$

and this remains non-zero in the infinite volume limit. This implies that in $D = 1 + 1$ there cannot be an infinitely sharp first order transition even in the large volume limit. However, because both σ_{cd} (probably) and f (certainly) grow $\propto N^2$, there can be a phase transition at $N = \infty$, and this can occur at finite volume.

Returning to our numerical results, we begin with $SU(12)$ and show in Fig. 25 how the average plaquette difference $\langle(u_{01} - u_{02})\rangle$ varies across the transition when we vary the ‘spatial’ volume, L_2 . (We expect the plaquette difference to be less sensitive to domain formation than the Polyakov loop.) It is clear that the transition does become much sharper when we pass from $L_2 = 10$ to $L_2 = 40$ although the nature of the change between $L_2 = 40$ and $L_2 = 80$ is less clear. The evidence is for a would-be first-order transition inhibited by the domain formation described in the previous paragraph.

Turning now to the N -dependence of the transition, we show in Fig. 26 how $\langle|\bar{l}_{\mu=1}|\rangle$ varies with γ on a $2 \times 4 \times 10$ lattice for $SU(6)$, $SU(12)$ and $SU(24)$ gauge theories. We see a rapid sharpening of the transition with increasing N which leaves little doubt that there is a first-order transition at $N = \infty$ at $L_2 = 10$, and presumably at other values of L_2 as well.

4.4.3 Third transition

To search for a third transition, characterised by a non-zero expectation value for $|\bar{l}_{\mu=2}|$, we take our $SU(12)$ gauge theory on an $2 \times 4 \times 10$ lattice and increase γ beyond the values associated with the transitions discussed above. In Fig. 27 we plot the resulting values of $\langle|\bar{l}_{\mu=2}|\rangle$. We see a transition of the kind that we are looking for, but one which is very smooth. Increasing N to $N = 24$ we see what appears to be a significant sharpening of the transition, suggesting that it might become an actual phase transition at $N = \infty$.

In Fig. 28 we show a histogram of the values of $|\bar{l}_{\mu=2}|$ obtained in $SU(24)$ on a $2 \times 4 \times 10$ lattice at $\gamma = 156.25$. This shows a clear peak at low values that one naturally interprets as belonging to the confined phase, and a further peak (or peaks) at larger values that one

naturally associates with the deconfined phase. This suggests that if this is a phase transition at $N = \infty$ then it is first order.

5 Conclusions

We have shown that there is a very close match in the behaviour of several observables across the bulk transition that separates strong and weak coupling in 2+1 dimensions, and the Gross–Witten transition in 1+1 dimensions. In particular the third derivative of the partition function, $C_3 \propto N^4 \partial^3 \log Z / \partial \beta^3$, appears to develop a discontinuity as $N \rightarrow \infty$, just as it does across the Gross–Witten transition, providing strong evidence for a third order transition in the large- N limit of $D = 2 + 1$ $SU(N)$ gauge theories.

When we expressed $\partial^3 \log Z / \partial \beta^3$ as a cubic correlator of plaquettes, we saw that the discontinuity arose from fluctuations of plaquettes at the same position. It is thus a genuine $N = \infty$ phase transition that arises from the $N^2 \rightarrow \infty$ degrees of freedom on each plaquette rather than from the collective behaviour of a large number of separated plaquettes. This motivated us to study the eigenvalue spectrum of the plaquette. We found that at the critical inverse 'tHooft coupling, $\gamma = \gamma_c$, the spectrum develops a gap at the boundary of its range $e^{i\alpha} = \pm 1$ and this gap grows as γ increases. While the gap formation does not, in itself, lead to a nonanalyticity in Z , it possesses a feature that does. At $\gamma = \gamma_c$ and for $N \rightarrow \infty$ the spectrum $\rho(\alpha)$ approaches its end-points with a vanishing derivative. This means that the extreme eigenvalues possess fluctuations that diverge compared to the $O(1/N)$ fluctuations of the eigenvalues in the bulk of the spectrum, and this is directly related to the singularity in the partition function. All these features are exactly the same as in the $D = 1 + 1$ Gross–Witten transition. In addition we find that there is a very close match in the behaviour of the plaquette eigenvalue density and in the ratio of plaquette eigenvalue fluctuations when we compare the transitions in $D = 2 + 1$ and in $D = 1 + 1$. Thus it would appear that the bulk transition in 2+1 dimensions is very much like the Gross–Witten transition.

However, there is clearly more than this going on. The Gross–Witten transition has no peak in the specific heat, but we see in 2+1 dimensions a clear peak that coincides with (or is very close to) the third order transition. The contribution from neighbouring or nearly neighbouring plaquettes appears to grow with N , indicating a possible second–order phase transition in the large- N limit. Whether this is due to a correlation length that diverges as $N \rightarrow \infty$ (we see a slight decrease in the lightest mass that couples to the plaquette when we go from $SU(6)$ to $SU(12)$) or to the plaquette fluctuations decreasing more slowly than $1/N^2$ at the critical point, is not clear at present. In any case, the fact that the correlations between nearby plaquettes behave as if due to a flux emerging from an elementary cube, suggests that the transition may be due to centre monopole(-instanton) and vortex condensation. It is therefore plausible that this (possible) second–order phase transition is connected to the line of specific heat peaks in the fundamental–adjoint plane found in $SU(2)$ [22], which may also become a line of second–order phase transitions in the large- N limit, and which, just as in $D = 3 + 1$ [19], can be understood in terms of condensation of Z_N monopoles and vortices. In $D = 3 + 1$ this phase structure is believed to lead to the observed first order bulk transition.

Our $N = \infty$ second-order transition would appear to be a manifestation of the same dynamics, but in one lower dimension. Numerical calculations that are both more accurate and extend to larger N are clearly needed here.

We have also investigated the sequence of finite volume transitions on $L_0 L_1 L_2$ lattices. We argued that when the tori are strongly ordered, $L_0 \ll L_1 \ll L_2$, these can be understood in terms of deconfinement, followed by high- T dimensional reduction as β is increased, followed by deconfinement in the reduced system, and so on. So the first transition, which is first-order for large N , occurs at $\beta = \beta_{c_0}$ where $a(\beta_{c_0})L_0 = 1/T_{c_0}$. Then as we increase β , and hence T , the system will eventually be dimensionally reduced, $L_0 L_1 L_2 \rightarrow L_1 L_2$ for $T \gg T_{c_0}$. This $L_1 \ll L_2$ system will undergo a deconfining transition when $\beta = \beta_{c_1} \gg \beta_{c_0}$ where $a(\beta_{c_1})L_1 = 1/T_{c_1}$. Due to the fragmentation of the high- T phase into domains (a feature of 1 spatial dimension) this transition is a finite cross-over at finite N . As $N \rightarrow \infty$ the domain ‘wall’ tension should diverge (probably as N^2), the domain structure will be suppressed, and the cross-over appears to become a genuine first order transition. At higher β and hence higher $T^{D=1+1}$, we can again expect dimensional reduction to occur $L_1 L_2 \rightarrow L_2$ at some $T^{D=1+1} \gg T_{c_1}$. and there is some evidence that the ‘infinitesimal’ $L_0 \times L_1$ system undergoes a transition at $a(\beta_{c_2})L_2 = 1/T_{c_2}$ with $\beta_{c_2} \gg \beta_{c_1}$.

The first of these finite volume transitions becomes a phase transition as $L_1, L_2 \rightarrow \infty$ at fixed N . It also becomes a phase transition at fixed L_1, L_2 as $N \rightarrow \infty$. The latter will occur even as $L_1, L_2 \rightarrow L_0$. The second transition, which is a deconfining transition in the $D = 1 + 1$ effective theory, is a sharp crossover at finite N and appears to be first-order. As we remarked above, an actual phase transition is not possible at finite N in 1 spatial dimension because of domain formation. However, as we pointed out, this does not preclude a first-order phase transition at $N = \infty$, as suggested by our numerical computations. Such a $N = \infty$ phase transition will continue to occur for $L_2 \rightarrow L_1$, and it may be that it also survives the $L_1, L_2 \rightarrow L_0$ limit, although we have not investigated this possibility. Finally we saw some numerical evidence for a third $N = \infty$ transition in the effective $D = 0 + 1$ theory, although here the calculations are no more than suggestive. These arguments can trivially be lifted to $SU(N)$ gauge theories in $3 + 1$ dimensions, where they clearly have some relation to the $N = \infty$ finite volume transitions on L^4 lattices transitions discussed in [2, 8, 7].

In view of conjectures [2, 8, 7] that Wilson loops in $D = 3 + 1$ may undergo $N = \infty$ non-analyticities, when their area, in physical units, reaches a critical value, we have analysed the behaviour of Wilson loops in $D = 2 + 1$ $SU(N)$ gauge theories. Our results show a remarkable match between the behaviour of Wilson loops in $D = 2 + 1$ and in $D = 1 + 1$, where a gap in the Wilson loop eigenvalue spectrum is known to open at a critical area at $N = \infty$, in both the lattice and continuum theories [9, 10]. We find that the eigenvalue spectra of Wilson loops (and indeed Polyakov loops) in $D = 2 + 1$ match those of Wilson loops in $D = 1 + 1$ when the traces are equal. Moreover the spectra of Wilson loops of any size (in lattice units and when larger than about 2×2) also match if the couplings are tuned to values where their traces are equal. This is true for any fixed N . As a corollary, it immediately follows that in $D = 2 + 1$ at $N = \infty$ a gap will form in the eigenvalue spectrum of a Wilson loop at a critical coupling that depends on the size of the loop. However because of a logarithmically divergent self-energy piece, this non-analyticity in the spectrum will not occur at a finite non-zero value

of the area in the continuum limit. This is in contrast to the case in $D = 1 + 1$. We have preliminary evidence [15] for a similar matching between Wilson loops in $D = 3 + 1$ and those with the same trace in lower dimensions. Here the self-energy divergence is even more severe and the gap forms deep in the ultraviolet. As in $D = 2 + 1$ one can imagine regularising this self-energy by using finite mass sources in constructing the ‘Wilson/Polyakov loops’, so as to obtain a gap formation at a fixed physical area.

The appearance of the gap at $N = \infty$ follows quite generally if we make plausible connections with Random Matrix Theory. The spectrum of an $l \times l = aL \times aL$ Wilson loop should be flat at large a , since linear confinement demands its trace to be $\propto \exp\{-\sigma l^2\} \sim 0$, while at sufficiently small a we expect to find the Wigner semi-circle of the $N = \infty$ Gaussian Unitary Ensemble. Somewhere in between a gap must form. Because the derivative of the spectrum diverges at its end-point, in contrast to the plaquette at the bulk transition, there are no anomalous fluctuations of the extreme eigenvalues and no non-analytic behaviour in the correlators that are related to derivatives of the Wilson loop with respect to the coupling. And indeed we find the traces of Wilson loops to be analytic in the coupling just as they are in $D = 1 + 1$. Thus the physical implications of this nonanalyticity in the eigenvalue spectrum remain unclear.

The remarkable similarity between the eigenvalue spectra of Wilson loops in different dimensions does not appear to have a simple explanation within Random Matrix Theory and merits a more careful and quantitative investigation than the one provided in this paper.

The $D = 2 + 1$ large- N phase structure that we have investigated in this paper can be understood, as we have argued above, in terms that appear to allow a unified understanding of these phase transitions in $D = 1 + 1$, $D = 2 + 1$ and $D = 3 + 1$ $SU(N)$ gauge theories.

Note added.

This revised version arose from our discovery, immediately after sending the original version to the archive, of the papers [9, 10] which then motivated our revised and extended study of Wilson loops in this paper. As this revision was in progress an interesting paper [30] on gap formation in smeared Wilson loops in $D = 3 + 1$ has appeared.

Acknowledgements

We are grateful to Barak Bringoltz and Helvio Vairinhos for useful discussions throughout this work and to Gernot Akemann for convincing us of the potential relevance of random matrix theory. We are also grateful to Rajamani Narayanan and Herbert Neuberger for discussions much earlier that sparked our original interest in these problems. Our lattice calculations were carried out on PPARC and EPSRC funded computers in Oxford Theoretical Physics. FB acknowledges the support of a PPARC graduate studentship.

References

- [1] D. Gross and E. Witten, Phys. Rev. D 21 (1980) 446.
- [2] R. Narayanan and H. Neuberger, *Plenary Talk at Lattice 2005*, hep-lat/0509014.
- [3] M. Campostrini, Nucl. Phys. Proc. Suppl. 73 (1999) 724 [hep-lat/9809072].
- [4] B. Lucini and M. Teper, JHEP 0106 (2001) 050 [hep-lat/0103027].
- [5] B. Lucini, M. Teper and U. Wenger, JHEP 0502 (2005) 033 [hep-lat/0502003].
- [6] B. Lucini, M. Teper and U. Wenger, JHEP 0401 (2004) 061 [hep-lat/0307017].
- [7] J. Kiskis, R. Narayanan and H. Neuberger, Phys. Lett. B574 (2003) 65 [hep-lat/0308033].
R. Narayanan and H. Neuberger, Phys. Rev. Lett. 91 (2003) 081601 [hep-lat/0303023].
- [8] R. Narayanan and H. Neuberger, in *Large N_c QCD 2004* (World Scientific, Ed. Goity et. al.) hep-lat/0501031.
- [9] B. Durhuus and P. Olesen, Nucl. Phys. B184 (1981) 461.
- [10] A. Bassetto, L. Griguolo and F. Vian, Nucl. Phys. B559 (1999) 563 [hep-th/9906125].
- [11] M. Teper, in *Large N_c QCD 2004* (World Scientific, Ed. Goity et. al.) [hep-th/0412005].
- [12] G. 't Hooft, Nucl. Phys. B72 (1974) 461, B75 (1974) 461.
- [13] M. Teper, Phys. Rev. D59 (1999) 014512 [hep-lat/9804008].
B. Lucini and M. Teper, Phys. Rev. D66 (2002) 097502 [hep-lat/0206027].
- [14] B. Lucini, M. Teper and U. Wenger, JHEP 0406 (2004) 012 [hep-lat/0404008].
- [15] F. Bursa, M. Teper and H. Vairinhos, PoS (LAT2005) 282 [hep-lat/0509092] and work in progress.
- [16] M. Creutz, *Quarks, gluons and lattices* (CUP, 1983).
- [17] G. Bhanot and M. Creutz, Phys. Rev. D 24 (1981) 3212.
R.W.B. Ardill, M. Creutz and K.J.M. Moriarty J. Phys. G 10 (1984) 867.
P. Stephenson, hep-lat/9509070, hep-lat/9604008.
- [18] T. Blum et al, Nucl. Phys. B442 (1995) 301 [hep-lat/9412038].
- [19] R. C. Brower, D. A. Kessler and H. Levine, Phys. Rev. Lett. 47 (1981) 621.
R. C. Brower, D. A. Kessler, H. Levine, M. Nauenberg and T. Schalk, Phys. Rev. D26 (1982) 959.
I. G. Halliday and A. Schwimmer, Phys. Lett. B101 (1981) 327; B102 (1981) 337.
L. Caneschi, I. G. Halliday and A. Schwimmer, Nucl. Phys. B200 (1982) 409; Phys. Lett. B117 (1982) 427.

- [20] Tien-lun Chen, Chung-I Tan and Xi-te Zheng, Phys. Lett. B109 (1982) 383.
- [21] G. Bhanot and M. Creutz, Phys. Rev. D 21 (1980) 2892.
P. Provero and S. Vinti, Mod. Phys. Lett. A6 (1991) 157.
- [22] M. Baig and A. Cuervo Nucl. Phys. Proc. Suppl. 4 (1988) 21.
- [23] K. Kajantie, M. Laine, K. Rummukainen and M. Shaposhnikov, Nucl. Phys. B503 (1997) 357 [hep-ph/9704416].
M. Laine and Y. Schroder, JHEP 0503 (2005) 067 [hep-ph/0503061].
- [24] Ph. de Forcrand and O. Jahn, hep-lat/0309153.
K. Holland, hep-lat/0509041.
J. Liddle and M. Teper, hep-lat/0509082.
- [25] P.Bialas, A. Morel, B.Petersson, K. Petrov and T.Reisz, Nucl. Phys. B581 (2000) 477 [hep-lat/0003004]; Nucl. Phys. B603 (2001) 369 [hep-lat/0012019].
P.Bialas, A. Morel and B.Petersson, Prog. Theor. Phys. Suppl. 153 (2004) 220 [hep-lat/0403020].
- [26] O. Aharony, J. Marsano, S. Minwalla, K. Papadodimas, M. van Raamsdook and T. Wiseman, hep-th/0508077
- [27] S. Coleman, 1979 Erice Lectures.
E. Witten, *Nucl. Phys.* **B160** (1979) 57.
A. Manohar, 1997 Les Houches Lectures, hep-ph/9802419.
Y. Makeenko, hep-th/0001047.
G. 't Hooft, in *Large N QCD*, Ed. R. F. Lebed (World Scientific, 2002) (hep-th/0204069).
- [28] M. Stephanov, J. Verbaarschot and T. Wettig, hep-ph/0509286.
- [29] T. Bhattacharya, A. Gocksch, C. Korthals Altes and R. Pisarski, Phys. Rev. Lett. 66(1991) 998; Nucl. Phys. B383 (1992) 497 (hep-ph/9205231).
P. Giovannangeli and C. P. Korthals Altes, Nucl. Phys. B608 (2001) 203 (hep-ph/0102022).
P. Giovannangeli and C. P. Korthals Altes, Nucl. Phys. B608 (2001) 203 (hep-ph/0102022); hep-ph/0412322.
C. Korthals Altes, A. Michels, M. Stephanov and M. Teper, Phys. Rev. D55 (1997) 1047 (hep-lat/9606021).
- [30] R. Narayanan and H. Neuberger, hep-th/0601210.

N	γ_c
2	0.700(3)
6	0.719(3)
12	0.722(2)
24	0.722(1)
48	0.722(2)

Table 1: Inverse coupling at which gap forms for 3×3 loops in $SU(N)$.

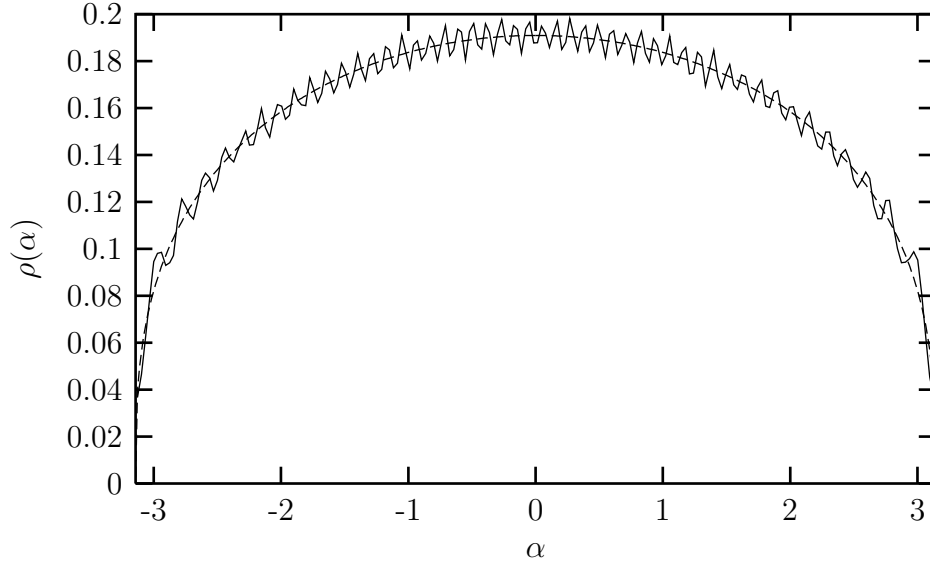


Figure 1: The spectrum of eigenvalues, $e^{i\alpha}$, of a 3×3 Wilson loop for $SU(48)$ in $D = 1 + 1$ at the critical coupling $\gamma = 1/\lambda = 1.255$, together with the continuum spectrum (---).

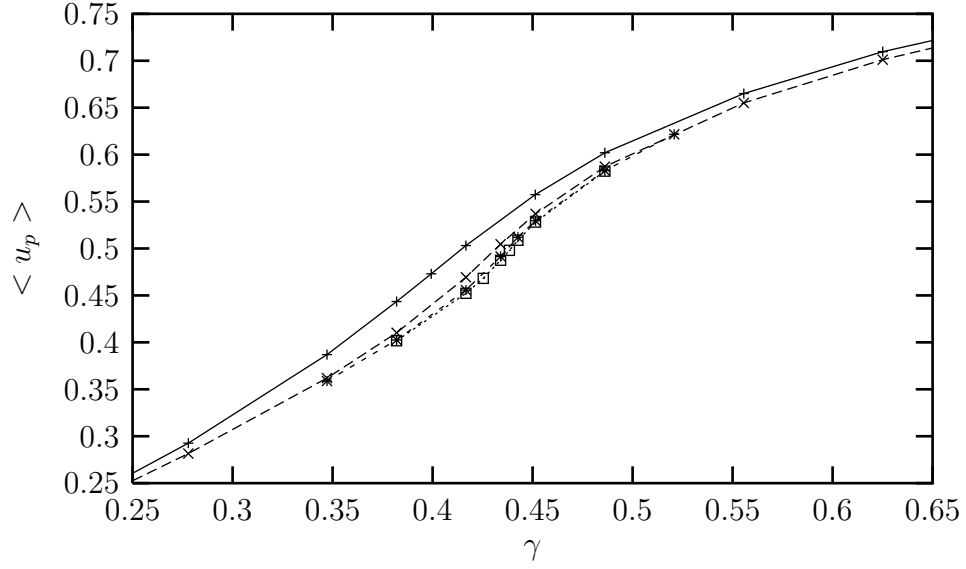


Figure 2: The average plaquette as a function of $\gamma = \frac{1}{ag^2N} = \frac{\beta}{2N^2}$ for SU(6) (+), SU(12) (x), SU(24) (*) and SU(48) (□).

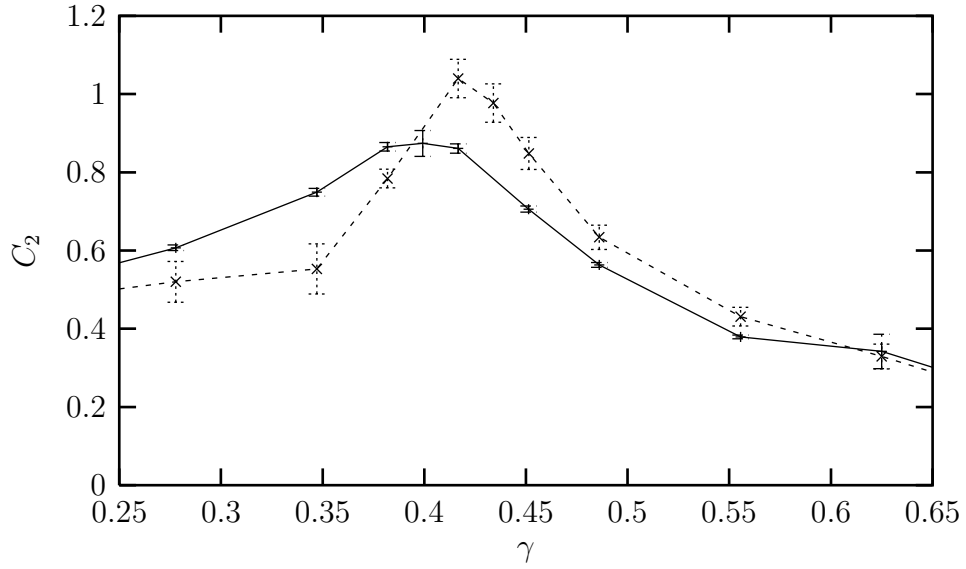


Figure 3: The specific heat, C_2 , as a function of $\gamma = \frac{1}{ag^2N} = \frac{\beta}{2N^2}$ for SU(6) (solid line) and SU(12) (dashed line).

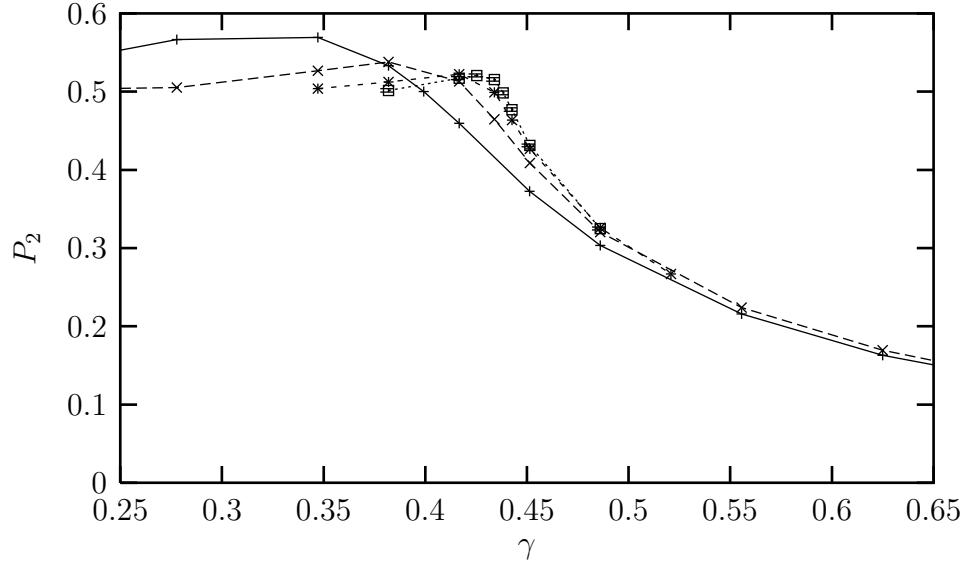


Figure 4: The ‘local’ specific heat, P_2 , as a function of $\gamma = \frac{\beta}{2N^2}$ for SU(6) (+), SU(12) (\times), SU(24) (*) and SU(48) (\square).

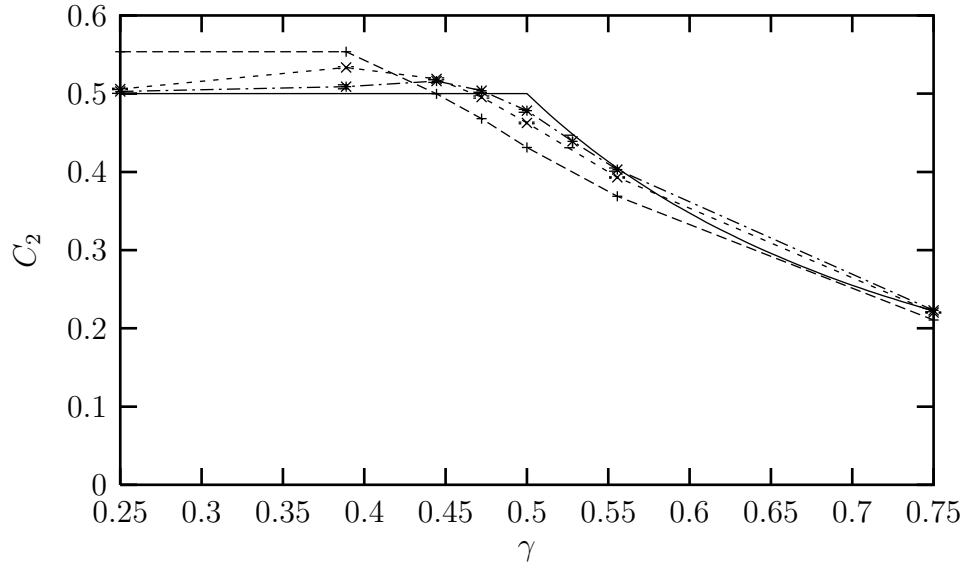


Figure 5: The specific heat, C_2 (equal to P_2 here) as a function of $\gamma = \frac{\beta}{2N^2}$ in 1+1 dimensions for SU(6) (+), SU(12) (\times), SU(24) (*) and the analytic result for SU(∞) (solid line).

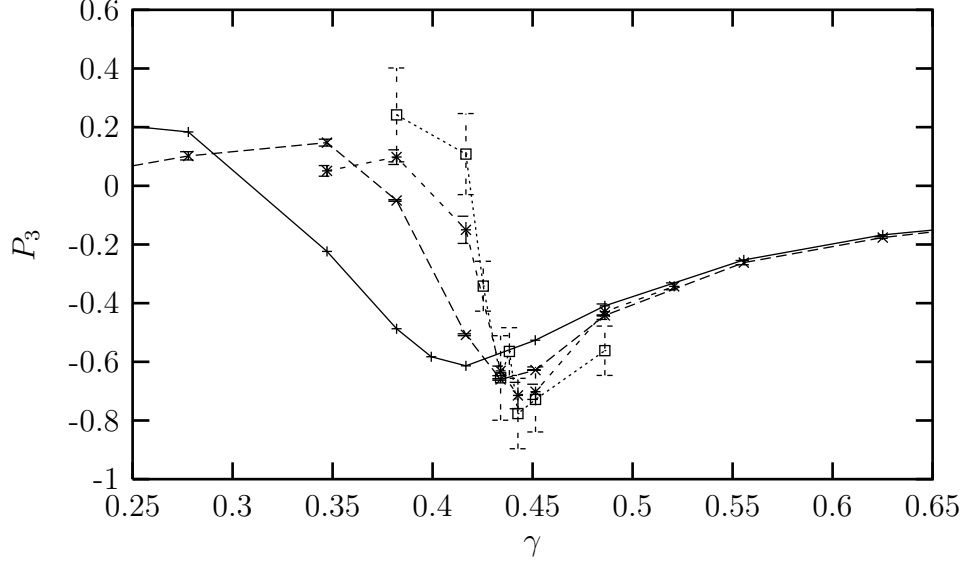


Figure 6: The cubic local plaquette correlator, P_3 , as a function of $\gamma = \frac{\beta}{2N^2}$ for SU(6) (+), SU(12) (\times), SU(24) (*) and SU(48) (\square).

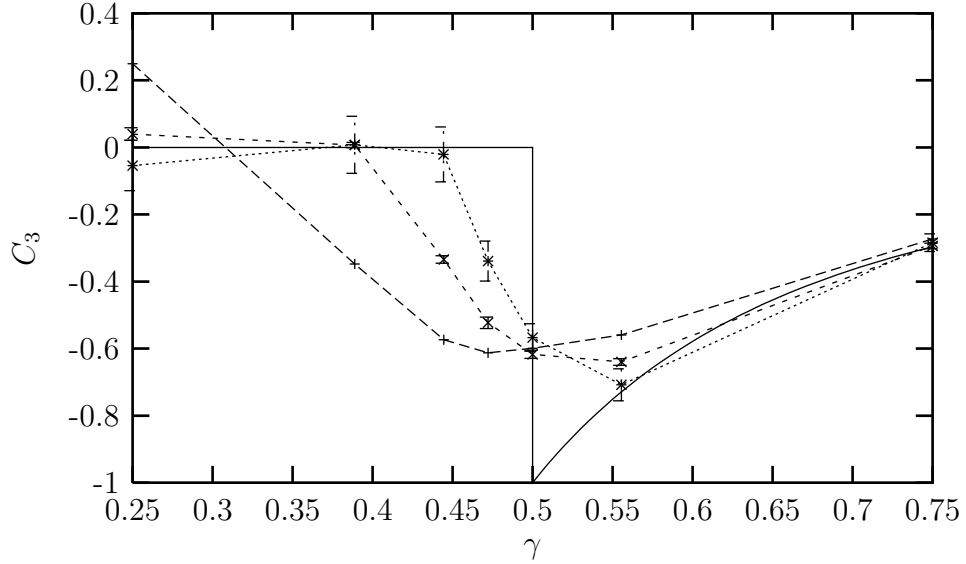


Figure 7: The cubic plaquette correlator, C_3 (equal to P_3 here) as a function of $\gamma = \frac{\beta}{2N^2}$ in 1+1 dimensions for SU(6) (long dashes), SU(12) (short dashes), for SU(6) (+), SU(12) (\times), SU(24) (*) and the analytic result for SU(∞) (solid line).

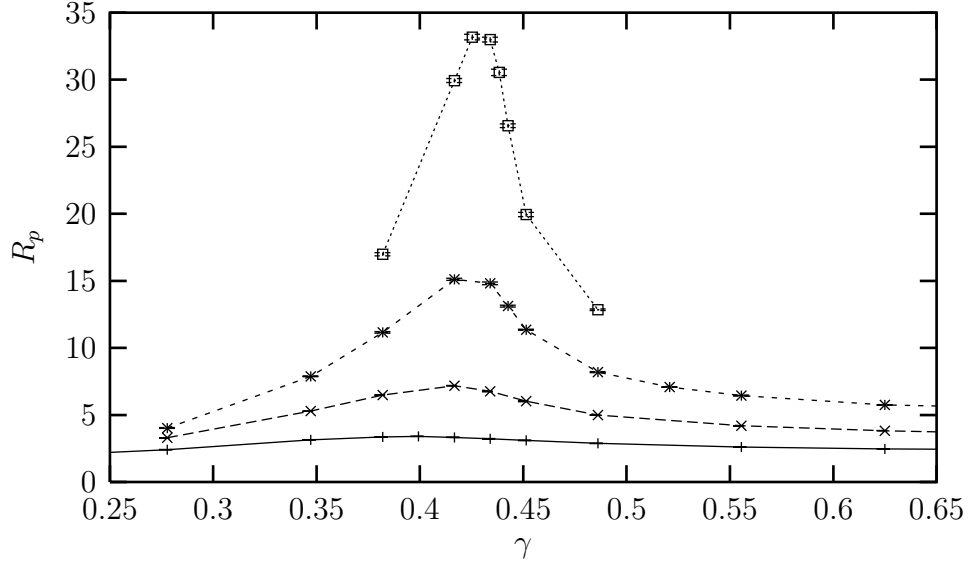


Figure 8: Fluctuations of extreme plaquette eigenvalues, R_p , as a function of $\gamma = \frac{\beta}{2N^2}$ for SU(6) (+), SU(12) (x), SU(24) (*) and SU(48) (□).

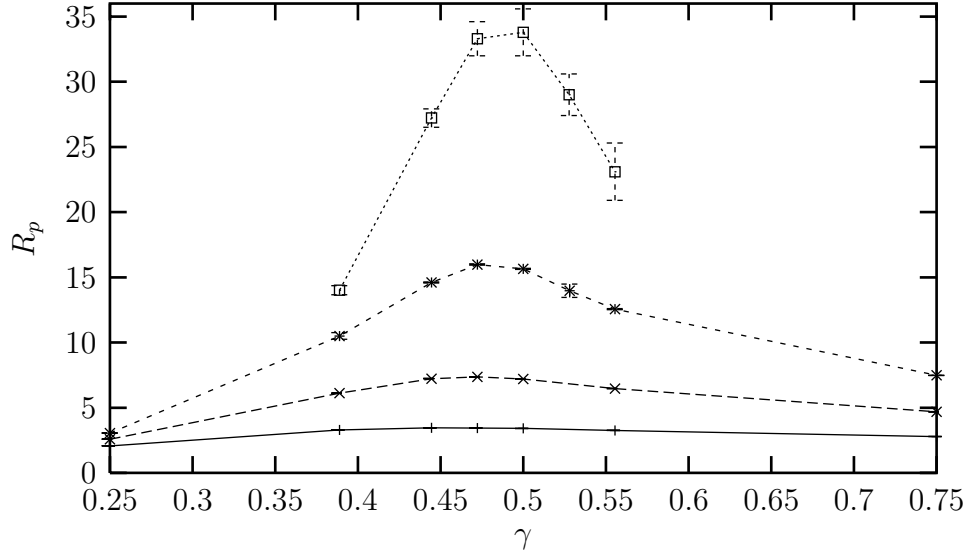


Figure 9: As in Fig. 8, but in 1+1 dimensions.

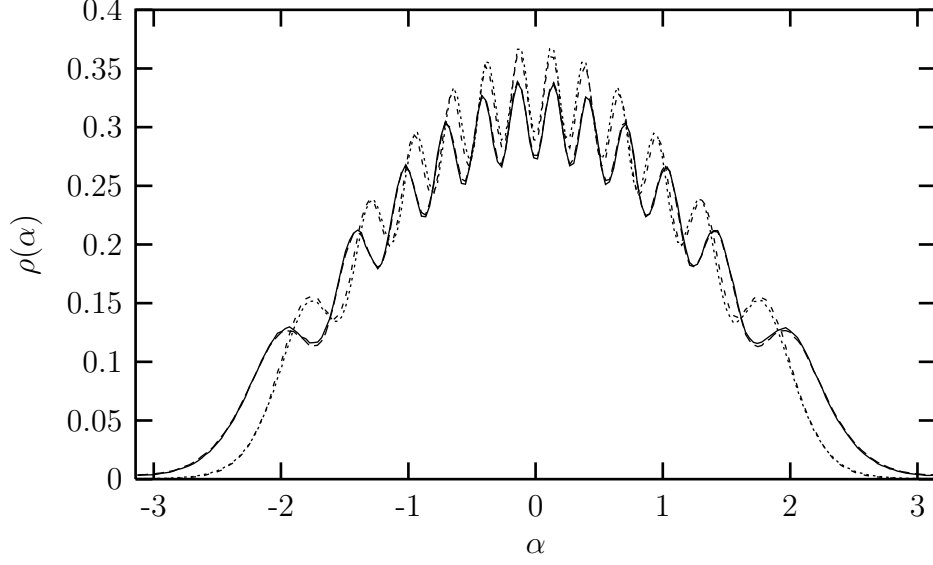


Figure 10: Density of plaquette eigenvalues, $e^{i\alpha}$, for SU(12) in 1+1 dimensions at $\gamma = \frac{\beta}{2N^2} = 0.462$ (long dashes) and $\gamma = 0.542$ (dots) and in 2+1 dimensions at $\gamma = 0.417$ (solid line) and $\gamma = 0.451$ (short dashes).

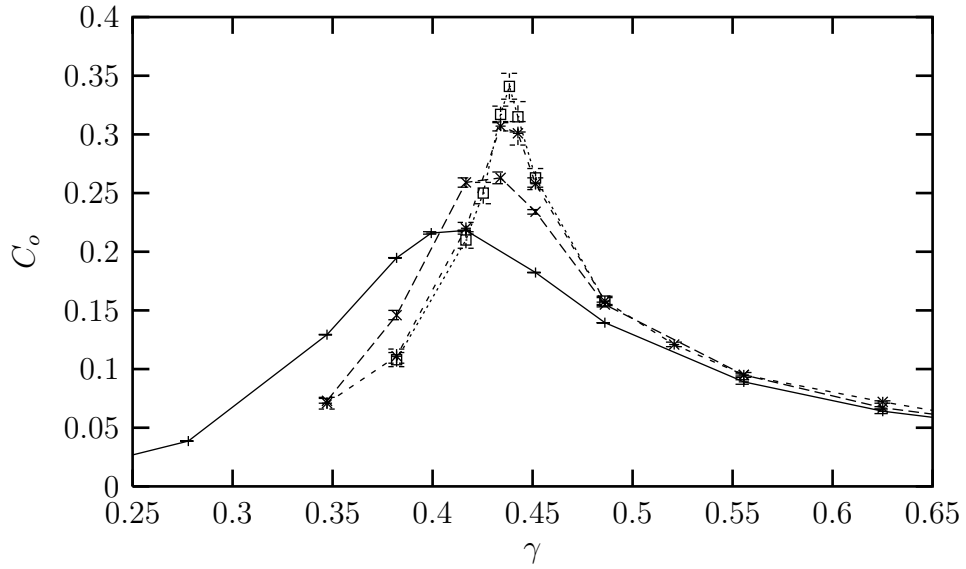


Figure 11: The plaquette correlator, C_o , as a function of $\gamma = \frac{\beta}{2N^2}$ for SU(6) (+), SU(12) (\times), SU(24) (*) and SU(48) (\square).

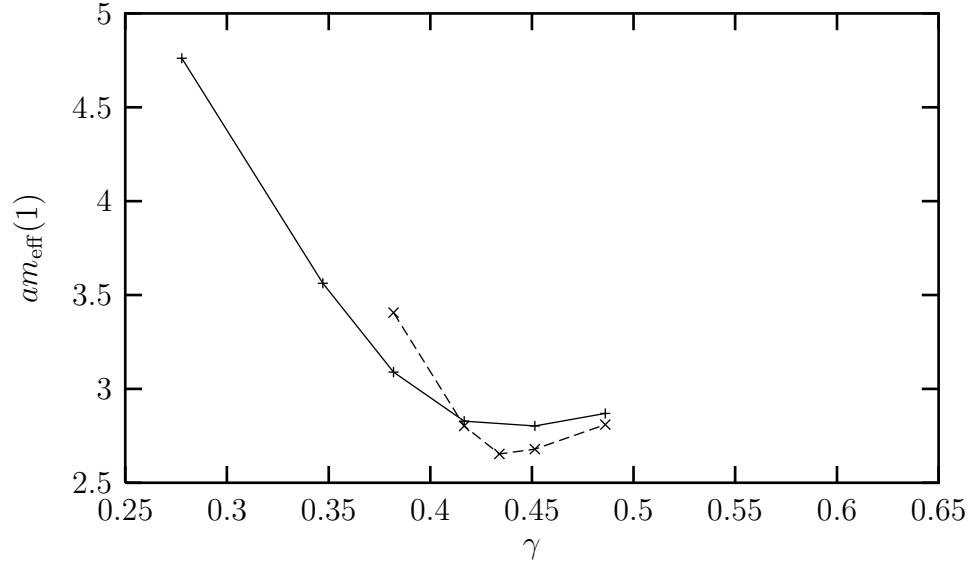


Figure 12: The lightest effective mass that couples to the plaquette as a function of $\gamma = \frac{\beta}{2N^2}$ for SU(6) (solid line) and SU(12) (dashed line).

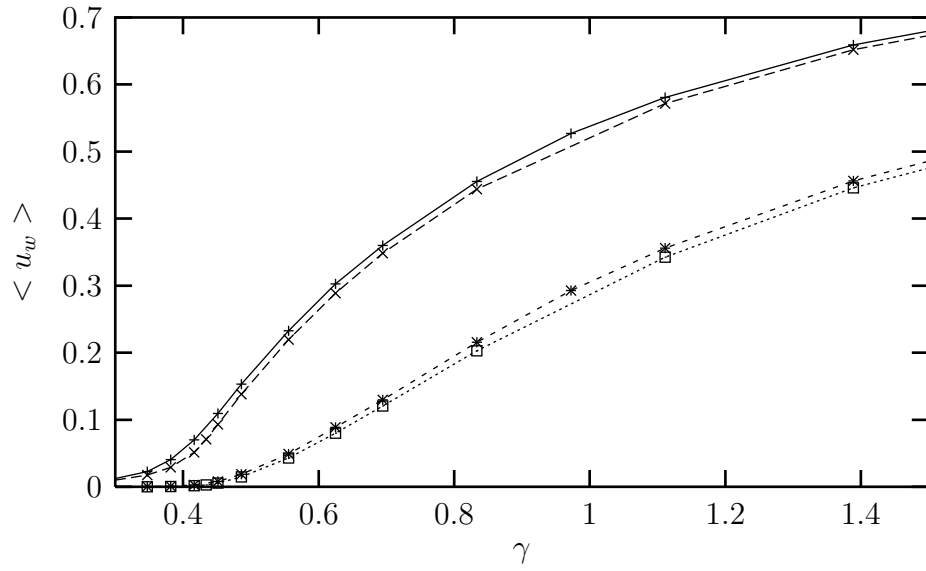


Figure 13: Trace of 2×2 Wilson loop in SU(6) (+) and SU(12) (x) and of the 3×3 loop in SU(6) (*) and SU(12) (square).

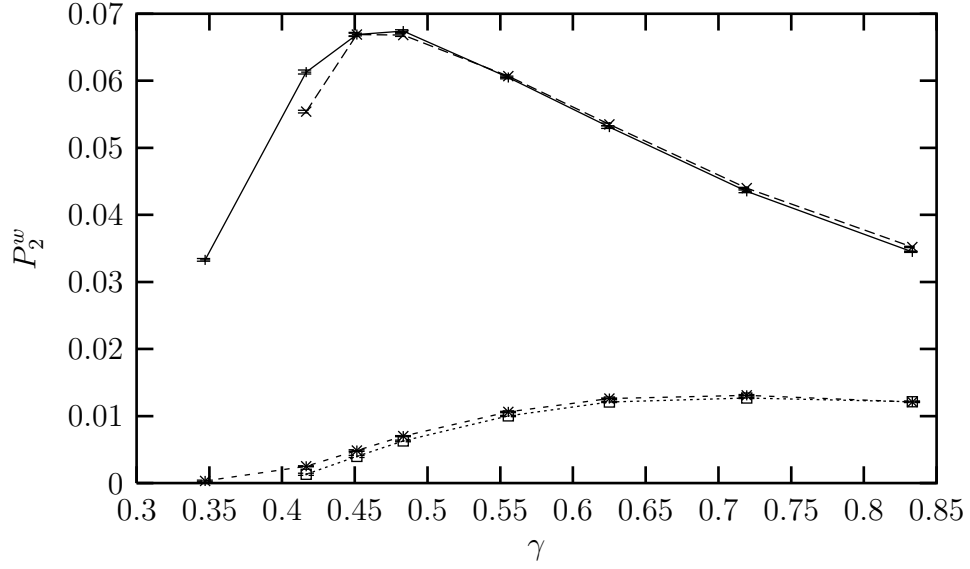


Figure 14: Local ‘specific heat’ of 2×2 and 3×3 Wilson loops in SU(6) and SU(12). Labels as in Fig. 13.

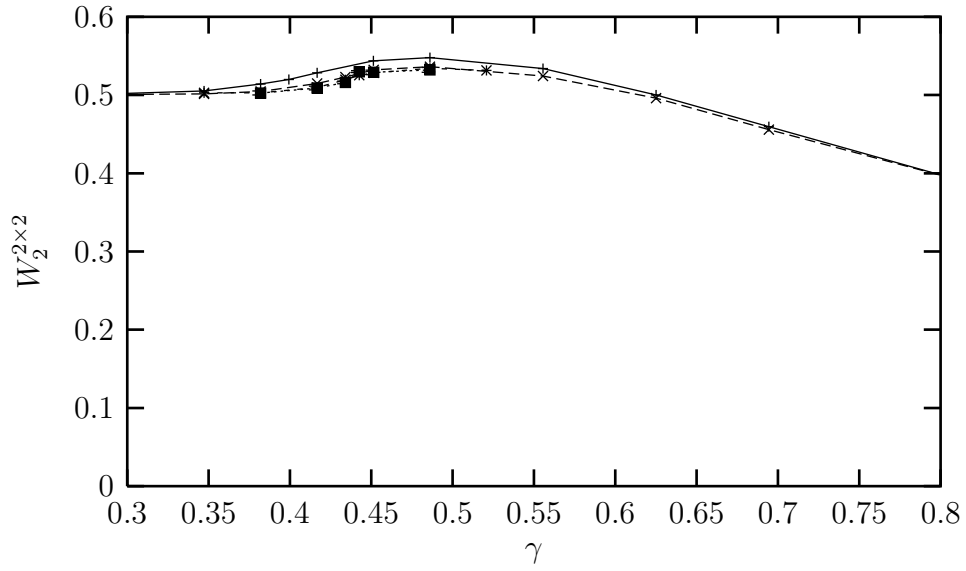


Figure 15: Quadratic correlator of 2×2 Wilson loops, $W_2^{2 \times 2}$, as a function of $\gamma = \frac{\beta}{2N^2}$ for SU(6) (+), SU(12) (x), SU(24) (*) and SU(48) (□).

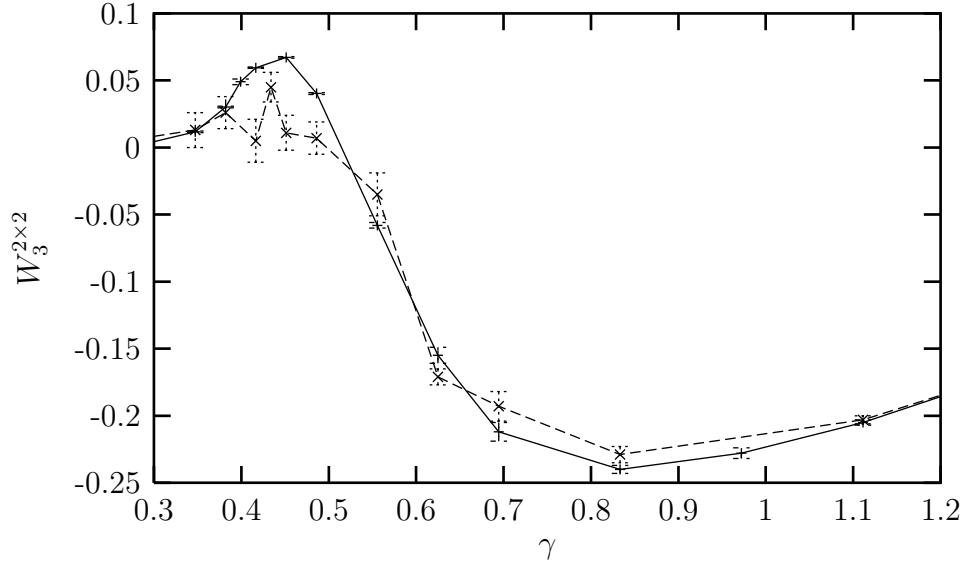


Figure 16: Cubic correlator of 2×2 Wilson loops, $W_3^{2 \times 2}$, as a function of $\gamma = \frac{\beta}{2N^2}$ for SU(6) (solid line) and SU(12) (long dashes).

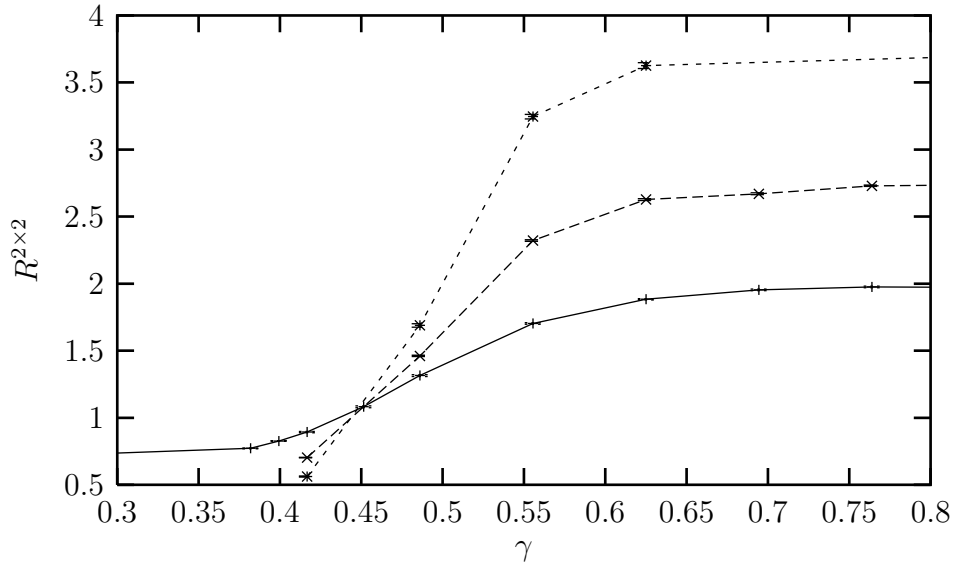


Figure 17: $R^{2 \times 2}$ as a function of $\gamma = \frac{\beta}{2N^2}$ for SU(6) (solid line), SU(12) (long dashes) and SU(24) (short dashes).

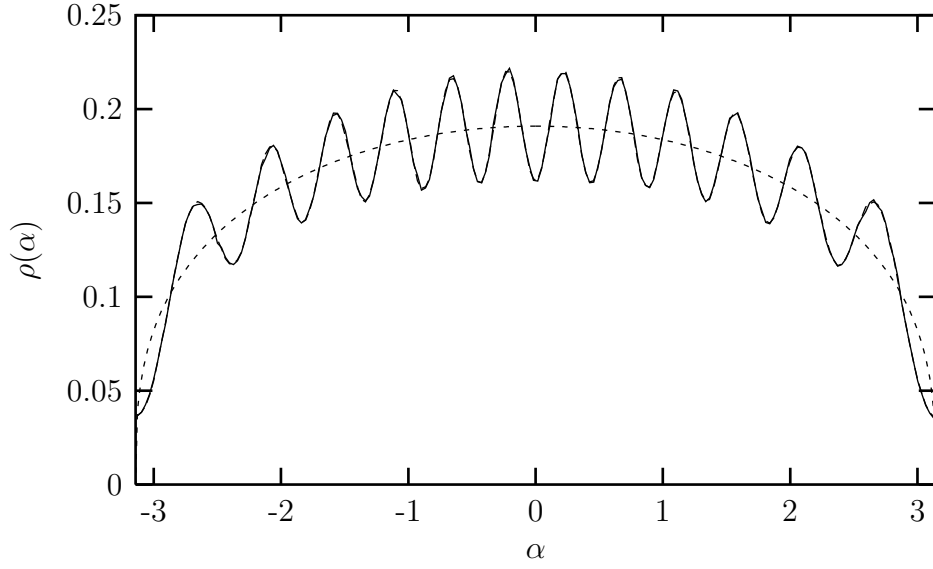


Figure 18: 3×3 Wilson loop eigenvalue density, $e^{i\alpha}$, for SU(12) in 1+1 dimensions at $\gamma = \frac{\beta}{2N^2} = 1.255$ (solid line) and in 2+1 dimensions at $\gamma = 0.722$ (long dashes), and the continuum large-N distribution in 1+1 dimensions at $A = A_{crit}$ (short dashes).

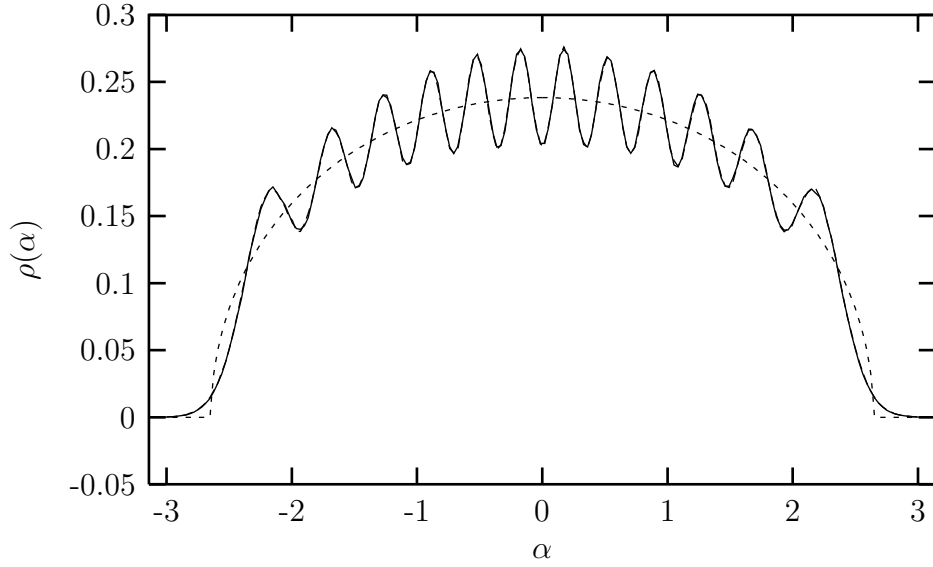


Figure 19: 3×3 Wilson loop eigenvalue density, $e^{i\alpha}$, for SU(12) in 1+1 dimensions at $\gamma = \frac{\beta}{2N^2} = 2.215$ (solid line) and in 2+1 dimensions at $\gamma = 1.111$ (long dashes), and the continuum large-N distribution in 1+1 dimensions at $A = 0.539A_{crit}$ (short dashes).

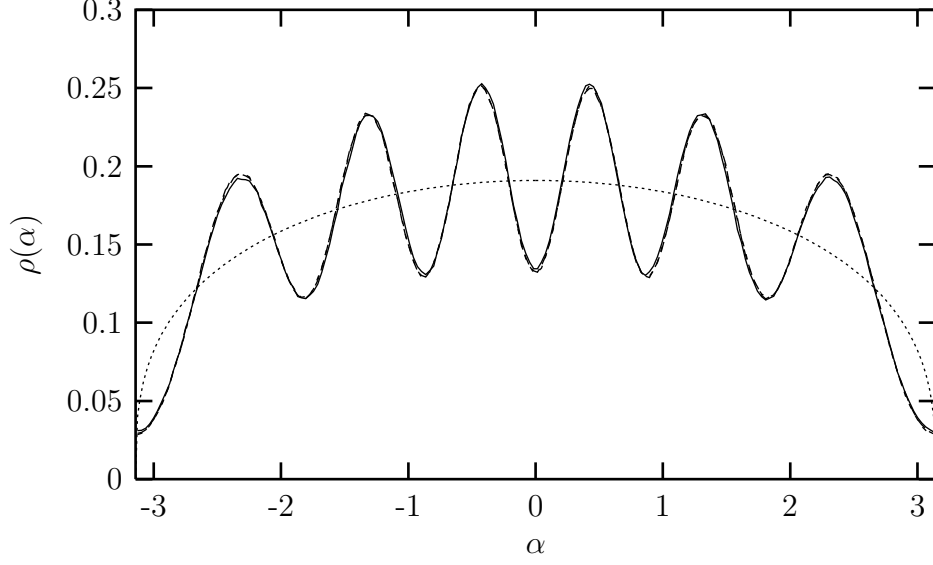


Figure 20: Eigenvalue density in $SU(6)$ in 2+1 dimensions for the 2×2 loop at $\gamma = 0.483$ (solid line), the 3×3 loop at $\gamma = 0.719$ (long dashes), the 4×4 loop at $\gamma = 0.965$ (short dashes) and the continuum large- N distribution in 1+1 dimensions at $A = A_{crit}$ (dots).

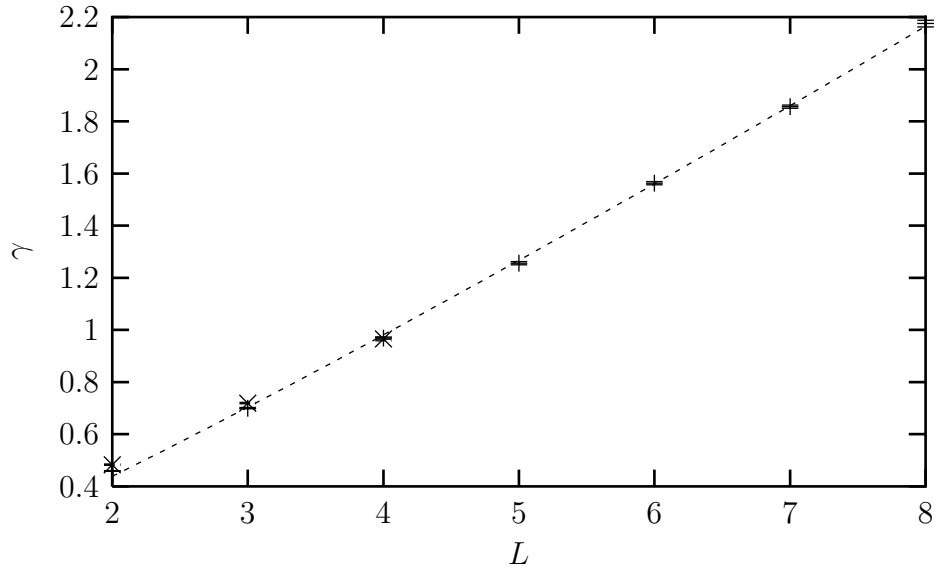


Figure 21: Couplings for which the gap forms for $L \times L$ Wilson loops in $SU(2)$ (+) and $SU(6)$ (*), and fit to $SU(2)$ data (dashed line).

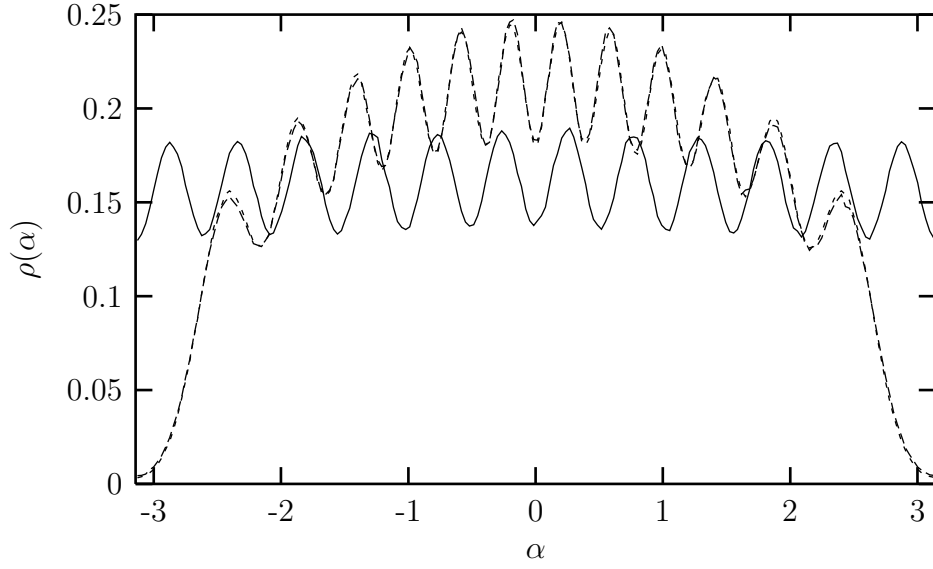


Figure 22: Polyakov loop eigenvalue density in SU(12) in 2+1 dimensions in the confined phase at $\gamma = 0.764$ (solid line) and in the deconfined phase at $\gamma = 0.833$ (long dashes), and the 3×3 Wilson loop in 1+1 dimensions at $\gamma = 1.684$ (dashes).

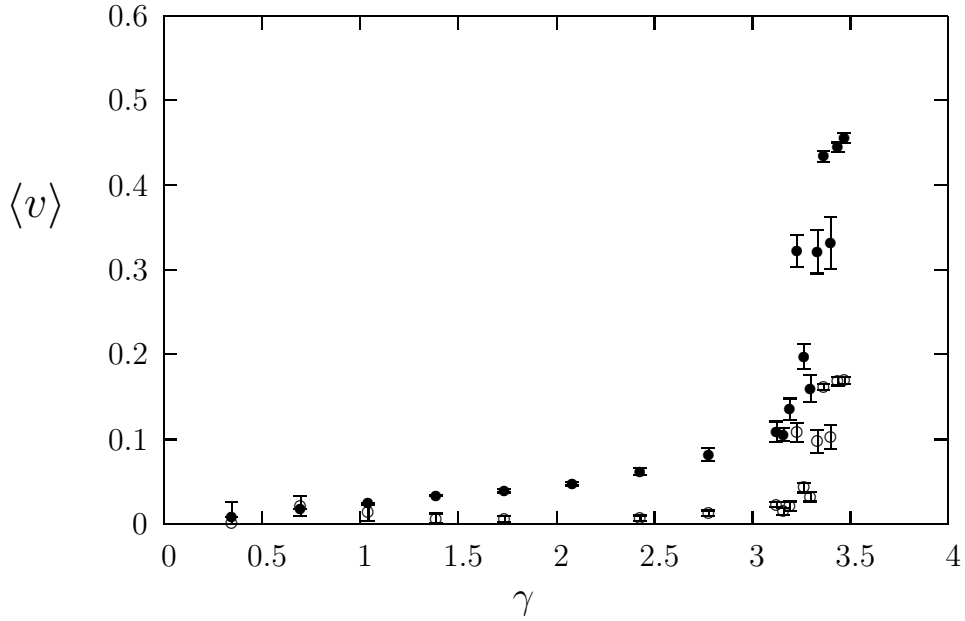


Figure 23: Values of the shorter 'spatial' Polyakov loop $\langle |\bar{l}_{\mu=1}| \rangle$, \bullet , and the plaquette difference $500 \times \langle (u_{01} - u_{02}) \rangle$, \circ , on a $2 \times 4 \times 40$ lattice in SU(12) versus the bare inverse 't Hooft coupling, $\gamma = \beta/2N^2$.

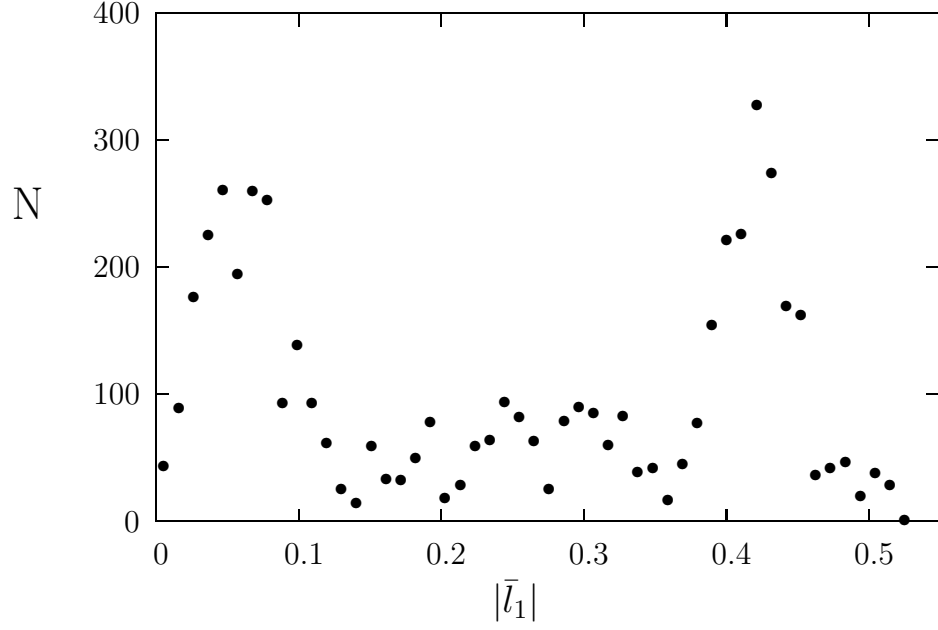


Figure 24: Histogram of values of the spatial Polyakov loop, $|\bar{l}_{\mu=1}|$, in SU(12) on a $2 \times 4 \times 80$ lattice at $\gamma = 3.368$.

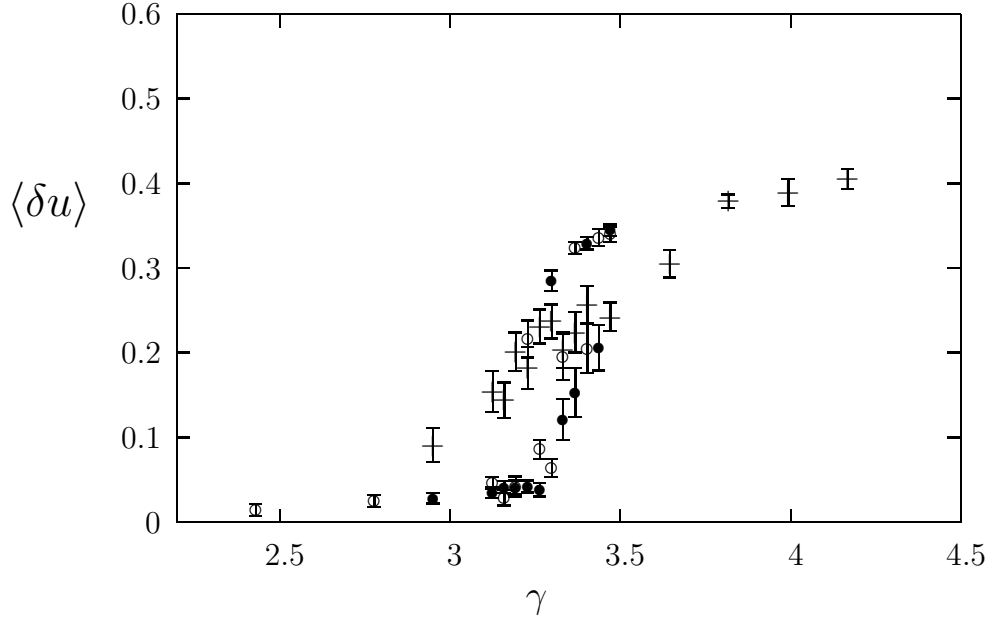


Figure 25: The average plaquette difference $\langle \delta u \rangle = 10^3 \times \langle (u_{01} - u_{02}) \rangle$ in SU(12) on $2 \times 4 \times L_2$ lattices with $L_2 = 10$ (+), $L_2 = 40$ (\circ), and $L_2 = 80$ (\bullet), versus $\gamma = \beta/2N^2$.

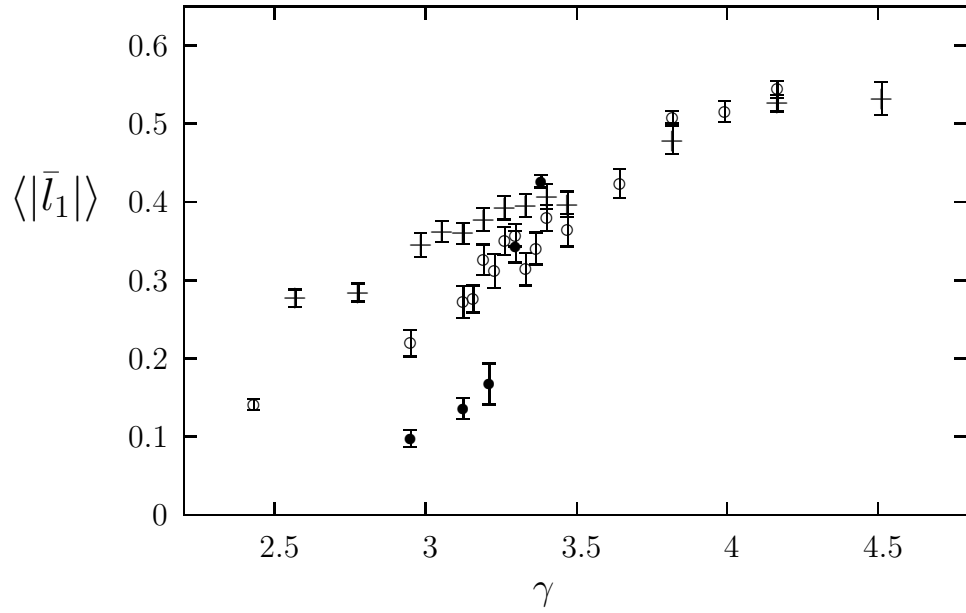


Figure 26: The average $\mu = 1$ Polyakov loop for $SU(6)$ (+), $SU(12)$ (o), and $SU(24)$ (•) versus the inverse bare 't Hooft coupling $\gamma = \beta/2N^2$, all on $2 \times 4 \times 10$ lattices.

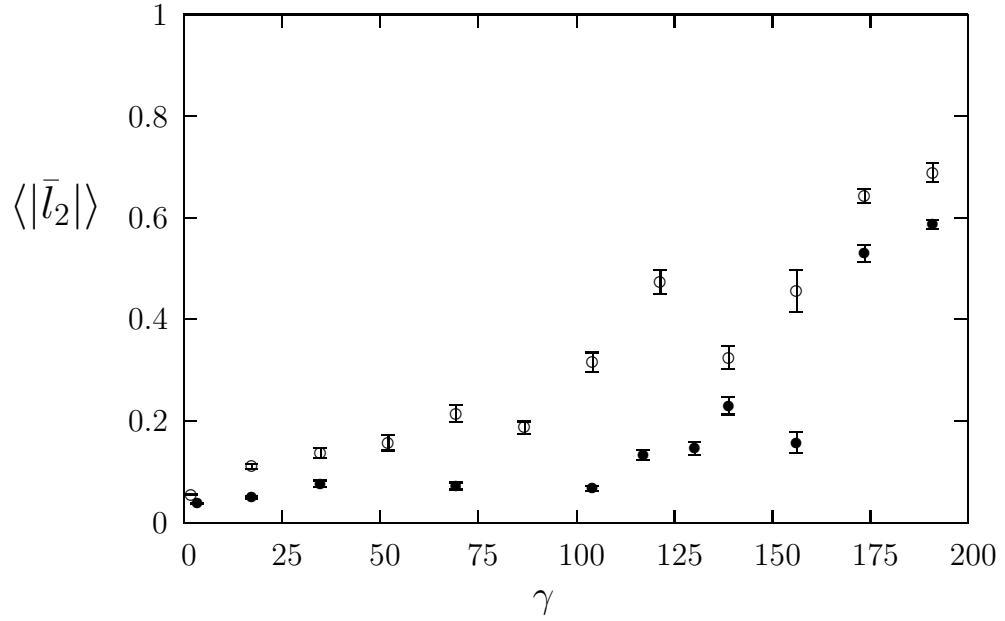


Figure 27: The average $\mu = 2$ Polyakov loop in $SU(12)$, o, and in $SU(24)$, •, on a $2 \times 4 \times 10$ lattice versus the inverse bare 't Hooft coupling $\gamma = \beta/2N^2$.

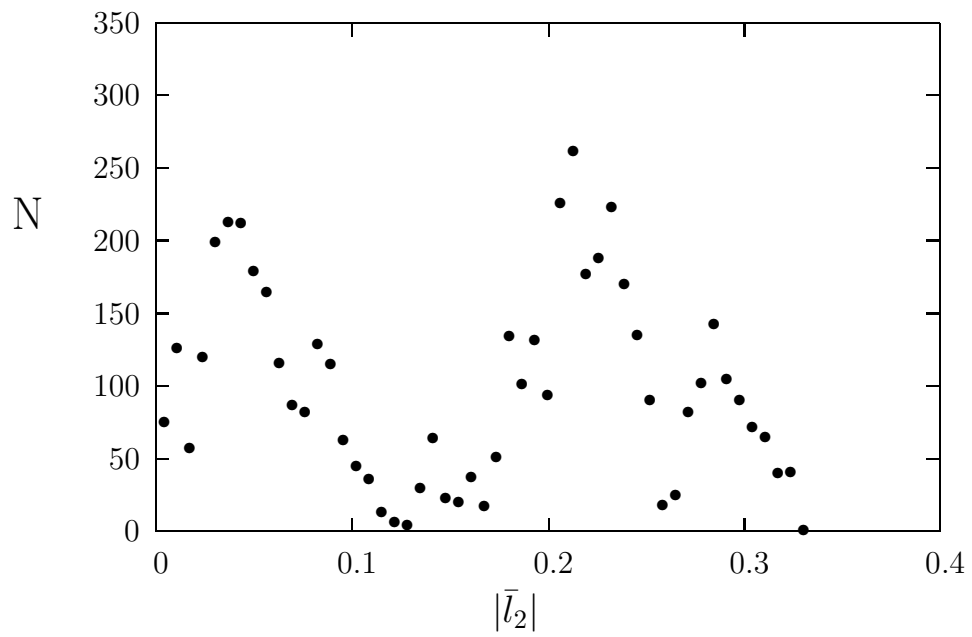


Figure 28: Histogram of values of $|\bar{l}_{\mu=2}|$ in SU(24) on a $2 \times 4 \times 10$ lattice at $\gamma = 156.25$.